The Effects of Secondary Air Injection on Particulate Matter Emissions

by

Joseph James Pritchard

B.S.E., Mechanical Engineering
University of Michigan, 2012

Submitted to the Department of Mechanical Engineering
in partial fulfillment of the requirements for the degree of

Master of Science in Mechanical Engineering

at the

MASSACHUSETTS INSTITUTE OF TECHNOLOGY

February 2014

Signature of Author.... .....
Department of Mechanical Engineering
January 17, 2014

Certified by.....
Wai K. Cheng
Professor of Mechanical Engineering
Thesis Supervisor

Accepted by.....
David Hardt, Professor of Mechanical Engineering
Chairman, Department Committee on Graduate Theses

To my parents

The Effects of Secondary Air Injection on Particulate Matter Emissions

by

Joseph James Pritchard

Submitted to the Department of Mechanical Engineering
on January 17, 2014 in partial fulfillment of the
requirements for the degree of
Master of Science in Mechanical Engineering

Abstract

An experimental study was performed to investigate the effects of secondary air injection (SAI) on particulate matter (PM) emissions. SAI was developed to reduce hydrocarbon (HC) emissions and has been shown to be effective as a strategy to reduce HC emissions at cold-start. In general, cold-start emissions have become an increasingly important problem due to new, more stringent vehicle emissions regulations. Direct-injection, spark-ignition (DISI) engines, which emit high levels of PM, are growing in popularity because of their fuel efficiency improvements. Meeting PM emissions becomes a more difficult task due to more stringent standards and the greater adoption of DISI engines. This study seeks to investigate the potential use of SAI to reduce PM emissions in the exhaust system.

Engine based experiments were conducted using a 2.0 L, turbocharged, DISI General Motors LNF engine. The engine was outfitted with a secondary air injection system and several thermocouples to measure exhaust stream temperature. A TSI Model 3934 Scanning Mobility Particle Sizer (SMPS) was used to measure particle emissions at various engine operating conditions and secondary air rates. PM reductions were observed for the engine conditions and SAI flow rates that were tested. The maximum particle number reduction achieved was 80%. Particle number and particle volume reduction were observed to correlate well with exhaust enthalpy release.

Thesis Supervisor: Wai K. Cheng
Title: Professor of Mechanical Engineering

Contents

List of Figures

List of Tables

Chapter 1: Introduction

Vehicle emissions have been regulated in the United States since the 1970s. One of the earliest pollutants to be regulated was hydrocarbon (HC) emissions. HC emissions led to the formation of smog, which was a primary concern associated with the growing use of vehicles. Later emissions regulations have been expanded to include standards for particulate matter (PM) emissions and vehicle fuel efficiency. The invention of the three-way catalyst is probably the single most important development in emissions reduction technology. It was proven to be very effective at reducing HC, carbon monoxide (CO), and nitrogen oxide (NOx) emissions.

A well-known concern regarding the use of catalysts is high emissions at cold-start. Before the catalyst reaches its operating temperature, it is mostly ineffective for reducing HC, CO, and NOx emissions. Currently, the majority of vehicle emissions measured during the federal test cycle occur during the first 25-30 seconds after engine start-up. As emission regulations continue to become more stringent, the significance of the cold-start emissions issue increases.

Secondary air injection (SAI) was proposed towards the beginning to the emissions regulation era as a strategy to reduce vehicle emissions. The basic theory was to inject air into the exhaust system to provide oxygen to enable the oxidation of HC and CO. Later versions of SAI sought to reduce emissions by quickening catalyst light-off. By enriching the engine mixture and injecting air into the exhaust it is possible to sustain an exothermic reaction within the exhaust system. This greatly increases exhaust gas temperature and heats the catalyst quickly. The effectiveness of SAI for reducing HC emissions has been well documented.

An aggravating factor for the cold-start emissions problem is the growing use of direct injection, spark ignition (DISI) engines. These types of engines have shown sizeable increases in fuel efficiency as compared to port fuel injected engines. DISI engines have led to higher HC and PM emissions, especially at cold-start, due to the

presence of liquid fuel within the cylinder. In light of increasingly more stringent HC standards and the DISI emissions issue, SAI has garnered some recent interest for its ability to reduce HC emissions at cold-start.

Until now, SAI has not been studied with respect to its potential for reducing PM emissions. Due to upcoming PM emissions regulations, and the growing use of DISI engines, innovative solutions to reduce PM emissions are needed. This study seeks to investigate the potential use of SAI as a way to reduce PM emissions at cold-start.

1.1 Background and Motivation

1.1.1 Health and Environmental Effects of Vehicle Emissions

The adverse effects of vehicle emissions on the environment and human health have been known for some time. These effects were the motivation behind emissions regulations beginning in the early 1970s. This study focuses on the effects of secondary air injection (SAI) on particulate matter (PM) emissions. SAI was originally developed as a strategy to reduce hydrocarbon (HC) emissions. Therefore, the focus of this background information will be HC and PM regulation. The primary adverse effect of HC emissions is the formation of smog. Sunlight causes HC in the atmosphere to participate in photochemical reactions which result in smog and ozone [1]. Regulation of HC has since helped to greatly reduce the presence of smog in urban areas with high vehicle emissions.

Particulate matter regulations are primarily in response to the negative health impacts of PM. The relation between PM and cardiovascular and respiratory issues has been extensively studied. The adverse effects of PM on respiratory function are well known and are especially impactful on people with pre-existing illnesses, such as asthma [2]. In light of the growing understanding of these health impacts, regulations of PM emissions have become increasingly more stringent.

1.1.2 Emissions Regulations for HC and PM

To address the health and environmental impacts of vehicles, emissions regulations were enacted, beginning with the Clean Air Act of 1970. Since then, air pollutants have been reduced by 72% despite total vehicle miles travelled increasing by 165% [3]. The initial vehicle emissions standards that resulted from the Clean Air Act went into effect in 1975. The pollutants regulated included carbon monoxide (CO), hydrocarbons (HC), and nitrogen oxides (NOx). HC emissions were limited to 1.5 g/mile, but there was no regulation for PM emissions [4]. In later years, the emissions standards became increasingly more stringent. For Tier I emissions standards, which were phased in beginning in 1994, the HC standard was reduced to 0.32 g/mile [5]. Tier II standards again lowered the HC standard to a maximum of 0.125 g/mile. Tier II standards were phased in from 2004 to 2009 and were the first instance of regulation of PM for gasoline powered vehicles. The PM limit was implemented on a mass basis and the maximum allowable emission for light-duty vehicles was 20 mg/mile [6]. The most recently enacted legislation was signed in 2013. It determined the Tier III standards which are to be phased in from 2017-2025. Tier III regulations enact a PM limit of 3 mg/mile for all light-duty vehicles and further reduces HC standards [7]. PM emissions regulations have also been enacted outside of the United States. The European Union has established both a particle mass and a particle number requirement. Particle mass has been limited to 4.5 mg/km. Particle number has been limited to $6.0 * 10^{11}$ particles/km [8]. The particle number is thought to be the more challenging standard to meet for DISI engines. This is because DISI engines tend to emit a high number of small diameter particles.

Emissions standards have continued to become more stringent since their inception in the 1970s. In addition to the pollutants listed above, there are also regulations on minimum fuel economy. Fuel economy standards have also continued to become more stringent. The combination of emissions and efficiency regulations has been a major driver of investment and innovation in the development of new passenger car engines. This has led to much research effort to develop new engine technologies.

1.1.3 History and Development of Secondary Air Injection

Innumerable engine technologies and control strategies have been investigated as potential ways to keep up with ever changing emissions standards. Probably the most successful and universally applied development was the three-way catalyst. Three-way catalysts were so named because they are able to simultaneously reduce concentrations of CO, NOx, and HC. They are most effective when the engine is operated at stoichiometric air-fuel ratios. The most significant drawback to the use of three-way catalysts is that they are mostly ineffective before they reach a temperature of about 250 °C [9]. This is part of what constitutes the cold-start emissions problem. The other factor that exacerbates the issue of cold-start emissions is the usual need to over-fuel to achieve an ignitable mixture in-cylinder [10]. This issue is primarily seen in port fuel injected engines. Due to high fueling rates and a cold catalyst, emissions during the first 25 seconds of engine operation constitute a majority of emissions seen during the entire FTP-75 test cycle.

Secondary air injection has been around for a long time in various forms. Generally, it can refer to a number of emission control strategies for which air is injected into the exhaust system. An early form of secondary air injection sought to preclude the need for a catalyst by injecting air during all engine operation [11]. Strategies can differ by where the air is injected and how the engine is operated to achieve a benefit with SAI. The strategy that has been the subject of research lately is designed to reduce hydrocarbon emissions, specifically at cold-start. This is achieved by using SAI to enable exothermic reactions in the exhaust, thereby speeding catalyst light off and reducing catalyst-in emissions. Typically, the engine is run with an enriched air-fuel mixture to provide combustible exhaust products. Spark timing is also retarded to increase exhaust temperatures. Air is then injected into the exhaust port to supply oxygen to react with the exhaust products. The exothermic reaction within the exhaust system serves to heat the catalyst and speed catalyst light-off. At the same time, catalyst-in emissions are reduced [12].

1.1.4 Engine-out Particulate Matter Emissions with Secondary Air Injection

During cold start, there are more in-cylinder liquid fuel films because low surface temperatures hinder evaporation. These fuel films are sources of PM emissions. Whelan et al. found a direct relationship between decreased engine body temperatures and increased PM emissions [13]. PM emissions are further enhanced by the SAI implementation strategy of engine enrichment and spark retardation. It is necessary to enrich the air-fuel ratio and to retard spark to provide the necessary exhaust products and temperatures to support heat release in the runner leading to the catalyst. Engine-out PM emissions are expected to increase due to enrichment. In a study by Sabathil et al., it was found that incomplete fuel oxidation at enriched engine conditions led to high PM emissions [14]. Another study also found that particle number was sensitive to small equivalence ratio changes [15]. In addition to equivalence ratio effects, it is expected that spark retardation will increase PM emissions. Chen et al. found that retarding the spark timing from an initial value of -20 degrees aTDC caused an increase in PM emissions. It was suggested that poor combustion at very late spark timings led to the increased PM emissions [16]. The spark timings used for SAI are typically much later than the timings used in the aforementioned study. Combustion performance will continue to degrade as spark timing is retarded and PM emissions will likely increase for very late timings with SAI.

1.1.5 Particulate Matter Composition and Oxidation

Of particular importance to this study is the potential for PM reduction with the use of SAI. The composition of PM is very important in determining the likelihood of PM reduction through oxidation. One study listed soot, ash, sulfates, and a soluble organic fraction (SOF) as components of PM in internal combustion engines. The SOF is basically hydrocarbon species from unburnt fuel. The study stated that soot and SOF are the primary components of PM [17]. Soot is composed mainly of carbon and SOF is typically referred to as volatile hydrocarbon species. Another study found that volatile

hydrocarbons constituted the majority of PM emissions by mass for a direct-injection, gasoline engine. The remainder of PM mass was given by soot [18].

The carbonaceous soot portion of PM emissions is known to be very difficult to oxidize at conditions found in the exhaust. Temperatures within the exhaust system are too low for fast oxidation of soot particles. Nagle and Strickland-Constable developed a formula for estimating soot oxidation rates for various temperatures and oxygen partial pressures [19]. This correlation has been shown to predict soot oxidation rates reasonably well [9]. Another study noted that soot oxidation was highly dependent on temperature and oxygen partial pressure. This same study also found that the Nagle and Strickland-Constable formula tended to overestimate soot oxidation rates, especially at lower temperatures [20]. The low temperatures considered by the study were relative to typical in-cylinder temperatures. These low temperatures were similar to the temperatures expected within the exhaust with SAI. The Nagle and Strickland-Constable formula was used to estimate soot oxidation rates at conditions that are typically seen within the exhaust with SAI. The resulting oxidation rate was much too low to achieve any significant oxidation of soot given the residence time of soot in the exhaust system. There is another aspect of soot oxidation that is relevant to the current study. This is the relationship between soot oxidation and the presence of hydroxyl radicals (OH). Numerous studies have shown that OH radicals are important in the oxidation of soot. This is due to the propensity for OH to react with carbon in soot and soot precursors [21]. The oxidation of combustible exhaust products with SAI should lead to the production of OH within the exhaust system.

Volatile hydrocarbon species are the other main component of PM emissions. This component is much more susceptible to oxidation than carbonaceous soot. Several studies have observed large reductions of PM across a catalyst. These reductions were attributed to oxidation of volatile particles in the catalyst. The first study reported a 94% reduction of particle number across the catalyst. This reduction was said to be due to the oxidation of volatiles. Some tests showed reductions across the entire particle size spectrum. The authors believed that volatiles existed as individual particles at

small sizes and volatiles were absorbed onto the surface of larger soot particles [22]. Another study noted a 65% reduction in particle number across the catalyst. Most of the reduction was due to the decrease in nucleation mode particles [23]. A third study found the highest reduction of particles in the catalyst was for particles in the range 5-50 nm. This was achieved at the slowest tested engine speed (1600 rpm) [24]. These studies all provide evidence of the oxidation of volatile species within the catalyst.

1.2 Research Objective

Substantial research effort has been made to study the effects of secondary air injection on hydrocarbon emissions at cold-start. SAI has been shown to be an effective way to reduce HC emissions through faster catalyst light-off. It is believed that no previous studies have been performed to investigate the effects of SAI on particulate matter emissions. An understanding of the potential effects of SAI on PM emissions could be of great use to automotive engineers as engines are adapted to meet increasingly more stringent emissions standards.

This study is intended to provide some insight into the evolution of PM emissions within the exhaust system during application of SAI. An experimental approach was taken to gather data on PM reductions. Tests were performed using an engine and dynamometer test cell. It was expected that PM emissions would increase due to the engine operating conditions necessary for using SAI. Additionally, it was thought that SAI could provide conditions within the exhaust system that would be conducive to reducing PM emissions. The experiments performed and the resulting data are thoroughly discussed in the following sections.

Chapter 2: Experimental Apparatus and Procedures

2.1 Experimental Setup

2.1.1 Engine Test Setup

The analysis of the effects of SAI on PM emissions was based on results of experiments performed using a 2.0L, turbocharged, DISI engine. The engine is a General Motors LNF Ecotec and is equipped with variable valve timing (VVT). The specifications of this engine are detailed below. The engine was coupled to a Froude-Consine AG-80 dynamometer. This dynamometer is absorbing only so the setup also included an electric motor mounted on the test bed.

Engine type	Turbocharged, In-line 4 cylinder
Displacement [cc]	1998
Bore [mm]	86
Stroke [mm]	86
Wrist pin offset [mm]	0.8
Connecting rod [mm]	145.5
Compression Ratio	9.2:1
Fuel system	Side-mounted gasoline direct injection
Valve configuration	16 valve DOHC, Dual cam phaser
Maximum torque	350 N*m at 200 rpm
Maximum power	260 kW at 5300 rpm

Table 2-1: Engine specifications

The engine control system consisted of two PCs. These computers were referred to as the "Master" and "Slave" computers. The desired operating parameters were input into the "Master" computer. These included engine RPM, spark timing, injection timing, injection duration, and valve timings. This information was then sent on to the "Slave" computer. The "Slave" computer then read engine sensors and sent control data to the engine. The control code run by the "Slave" computer was written in C at MIT.

The engine test cell was designed to be used for several different projects and therefore had the capability to replicate many different engine running conditions. There were two separate coolant circuits: one included a chiller and allowed for steady-state tests with cold coolant, the other included a heater and cold water heat exchanger to emulate coolant conditions from cold-start to fully warmed up. Additionally, the intake air system included an electric heater and an air-to-liquid heat exchanger. This setup allowed for the intake air temperature to be controlled across a range of temperatures. The intake air cooler also was used to reduce the humidity of the intake air.

The engine's fuel system was designed to allow for control of fuel temperature and supply pressure over a large range of values. The original, mechanical fuel pump was not used and instead an accumulator and pressurized nitrogen cylinder were used to contain and pressurize the fuel. This system uncoupled the fuel pressure from the engine operating conditions and allowed a constant, specified fuel pressure to be maintained.

A large array of sensors and thermocouples provided the necessary data to operate the engine and to perform analysis. A Kistler 6125A pressure transduced was used to measure the in-cylinder pressure for cylinder #4. Other pressure transducers measured MAP, fuel pressure, and exhaust pressure.

Type-K thermocouples were used throughout the engine setup to monitor and record various temperatures necessary for engine operation and data analysis. Intake air temperature was measured after the intake air heater and in the intake manifold. Coolant temperature was measured at the inlet and outlet of the engine block. Oil temperature was measured at the inlet and outlet of the oil pan. The fuel temperature was measured in the fuel line just before entering the fuel rail. Of particular importance to this work were the temperatures throughout the exhaust system. These measurements were very important to quantifying the effectiveness of oxidation in the exhaust with SAI. Five thermocouples were placed throughout the exhaust system and their locations are shown in Figure 2-1.

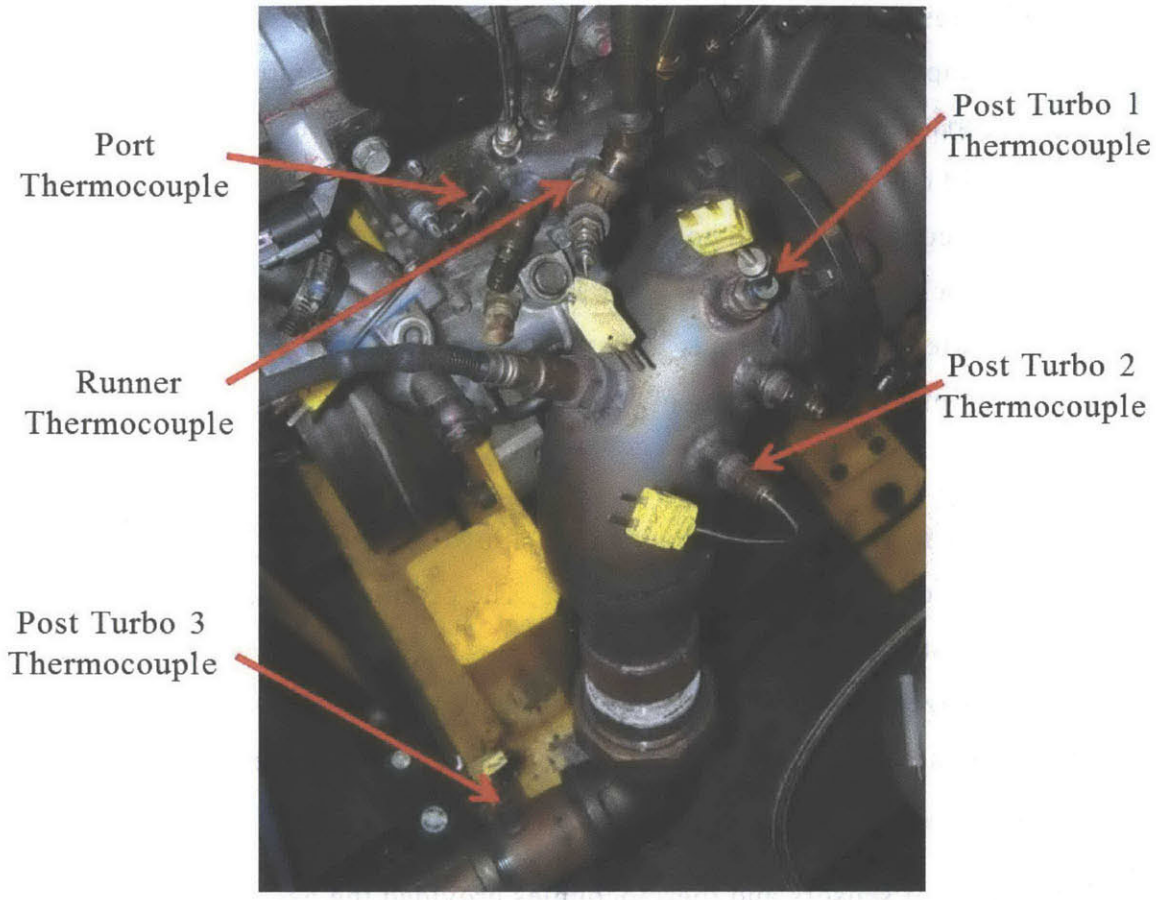

Figure 2-1: Exhaust thermocouple locations

The Port and Runner thermocouples are both equipped with aspirated radiation shields. The design of the radiation shields is shown in Figure 2-2. The aspirating flow is driven by the pressure differential from the exhaust manifold to atmospheric pressure. Exhaust gas was drawn down the inside of the tubular shield and then exited through a tee-fitting. The thermocouple ran down the center of the tubular radiation shield. This feature helped reduce conduction losses by exposing a substantial length of the thermocouple to the aspirating flow. The tip of the thermocouple was recessed 0.25 inch inside the radiation shield.

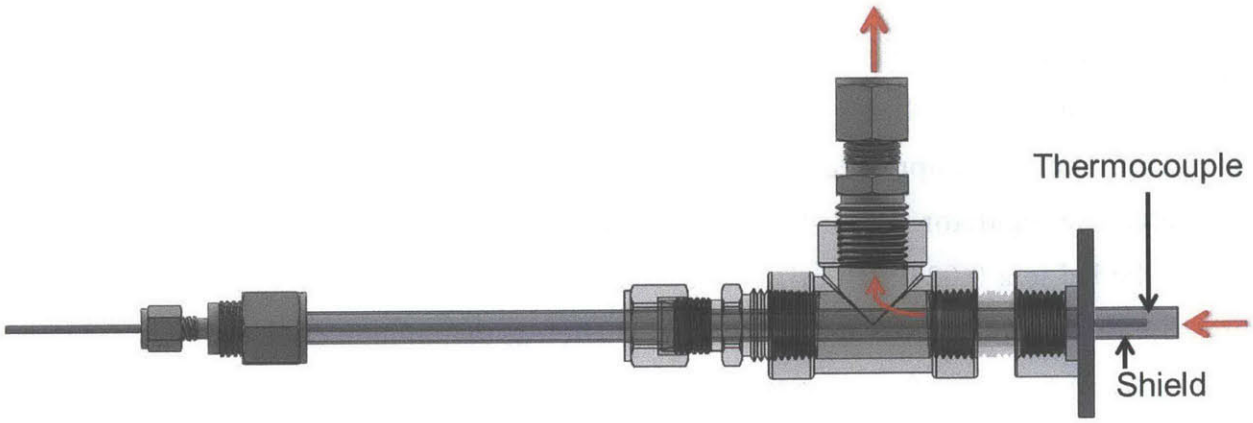

Figure 2-2: Aspirated radiation shield diagram

The air/fuel ratio of the engine was measured in the exhaust, downstream of the turbo. It was installed into an empty housing that took the place of the catalyst. All testing was done without a catalyst. The sensor used was an ETAS LA-4 UEGO. Because the sensor was located downstream of the turbo it measured an average value for all four cylinders. This lambda sensor was the primary way to adjust the rate of secondary air flow. The secondary air rate was typically increased until the lambda meter gave the desired value for lambda measured in the exhaust.

Exhaust gas was analyzed using a Horiba MEXA-584L Non-Dispersive Infrared (NDIR) analyzer. This instrument measures exhaust gas on a dry basis so the sample was dehumidified using a condenser and desiccant. The analyzer provided measures of CO2, CO, and hydrocarbon concentrations. The exhaust gas measured by the Horiba NDIR was not diluted before measurement. A Li-Cor LI-820 NDIR CO2 analyzer was used to measure the CO2 concentration in the diluted exhaust sample that was drawn through the particle sampling instrument. The dilution ratio for the particle sample could be determined by comparing the CO2 concentrations given by the two NDIR instruments.

2.1.2 Secondary Air Injection System

A secondary air injection system was designed and installed on the engine. Secondary air was supplied at each of the exhaust valves (eight in total). The system used a cylinder of compressed breathing air and a regulator to supply air at a steady pressure. The regulator fed air to a manifold that split the flow of air into eight tubes. Each tube led to a 0.023 inch orifice that regulated the flow of air into the exhaust. The pressure differential across the orifice was sufficient to maintain choked flow for all SAI rates. At the exit of each orifice, air entered $1/8^{th}$ inch stainless steel tubing that directed the air into each exhaust port. Each of these $1/8^{th}$ inch tubes entered the exhaust manifold through a Swagelok tube fitting in the exhaust runners. The tubes were sized and bent as to place the outlet as close the back of the exhaust valve as possible. This is important to facilitate mixing of the exhaust gas and the secondary air in the exhaust port. The location of air injection has been found to have a sizeable effect on SAI performance [25]. To promote mixing and prevent the stoppage of air flow during blowdown, the ends of the tubes were capped and drilled perpendicularly. The layout of the injection tubes relative to the exhaust valve is show in Figure 2-3.

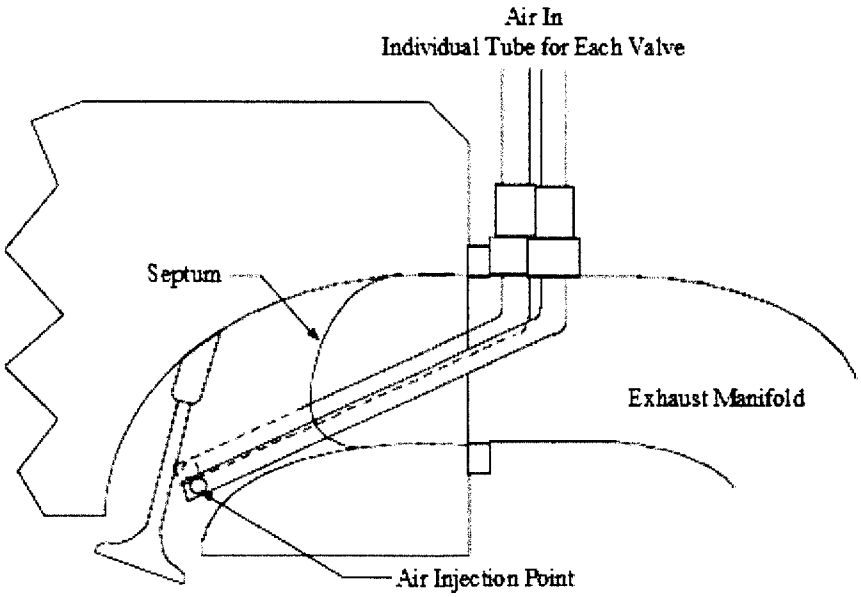

Figure 2-3: Secondary Air Injection Tube Location [26]

2.1.3 Particle Measurement

Particle emissions were measured using a TSI Model 3934 Scanning Mobility Particle Sizer (SMPS). This system is made up of a Model 3071A Electrostatic Classifier and a Model 3010 Condensation Particle Counter (CDC). The Electrostatic Classifier separates the particles by only allowing particles of a particular size to pass on to the CDC. The CDC then counts the particles within a particular size bin. Working in conjunction, the instruments measure the number of particles of a particular size and produce a particle distribution plot. Each measurement takes 90 seconds because of the time required to sweep the entire particle size distribution. For this reason, particle emission measurements using the SMPS can only be done at steady-state engine operation. The sample for particle measurement was drawn from the exhaust system about one meter downstream of the turbo. This was chosen to allow adequate time for any SAI oxidation to take place before the sample was drawn. It also allowed for the exhaust gas from each of the four cylinders and the secondary air to become well mixed before measurement. Cartridge heaters were used to heat the sample lines to prevent particle nucleation.

Before an exhaust sample may be analyzed, it must be diluted. This is necessary to ensure that the particle concentration is low enough that the SMPS can accurately measure it. Dilution also serves to reduce the hydrocarbon concentration and therefore reduce the possibility for nucleation of volatile particles. The dilution is achieved by mixing the exhaust sample with nitrogen. A dilution system that was designed for a previous project was used in this study. It consisted of a heated dilution block and a dilution tunnel. A diagram of the dilution block can be seen in Figure 2-4. The orifice between the exhaust flow and the sample chamber isolates pressure oscillations in the exhaust system. The sample chamber is maintained at atmospheric pressure. The measurement sample is drawn by a slight vacuum from the sample chamber into the dilution tunnel. Nitrogen is added to the sample within the dilution tunnel. The block and the sample tube are both heated to about 200 C to prevent nucleation of particles by condensation of hydrocarbons.

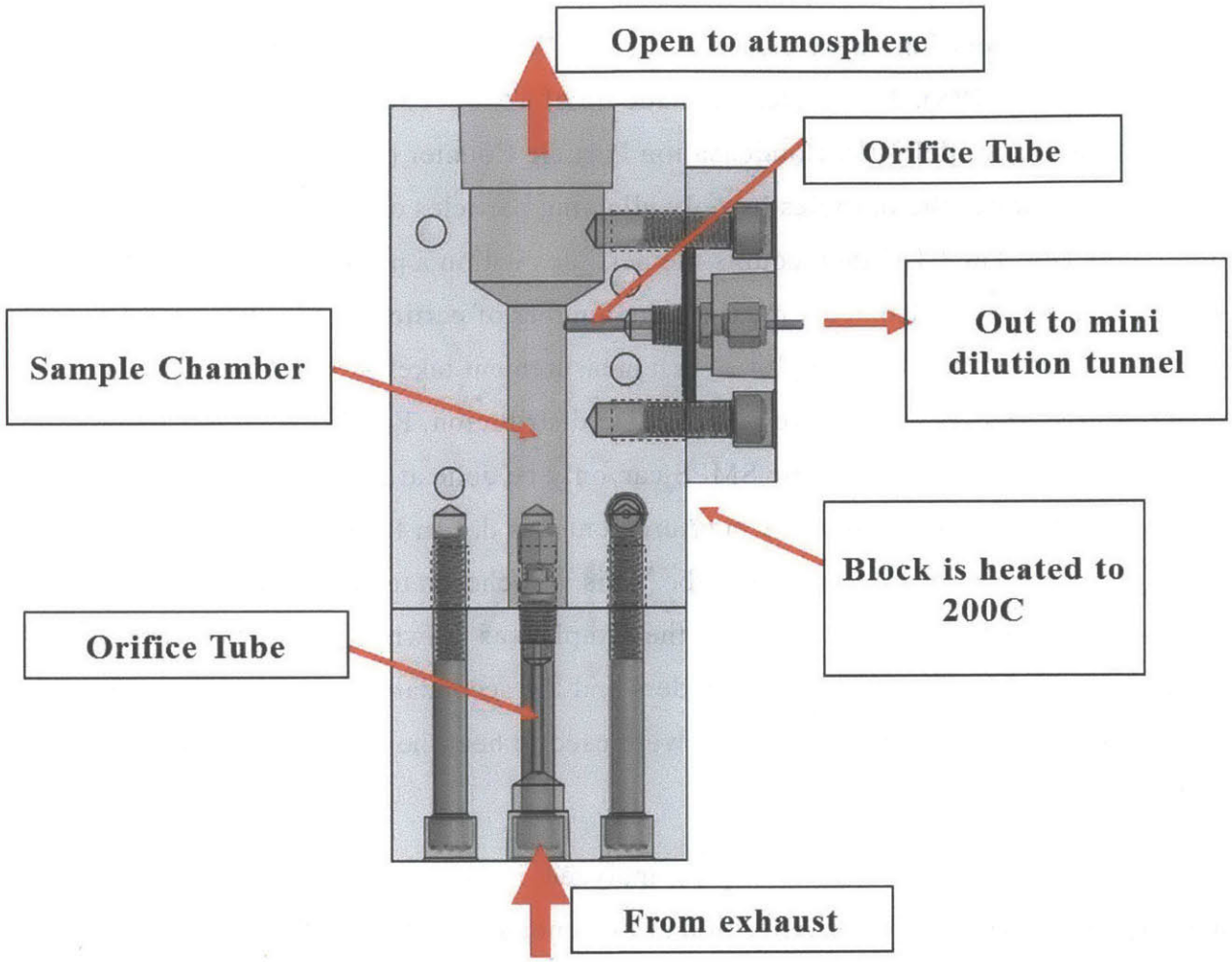

Figure 2-4: Dilution block diagram [27]

2.2 Experimental Conditions and Procedure

2.2.1 Test Conditions

All the data used in this study were obtained from tests performed using the previously described GM LNF engine. The tests were performed at steady state engine operation as necessitated by the length (90 seconds) of the SMPS particle measurement sweep. Efforts were made to simulate cold-idle conditions because SAI is most commonly used during engine cold-start. The efforts to simulate cold-idle pertained

mainly to engine speed, engine load, and fluid temperatures. To facilitate oxidation with secondary air, it was necessary to run with very late spark timing and highly enriched fuel mixtures. The engine conditions for cold-idle were defined by a previous student along with the industrial sponsors. These conditions are summarized below.

Engine Parameter	**Value**
Engine Speed [rpm]	1200
NIMEP [bar]	2
External EGR [%]	0
Coolant Temperature [C]	20
Oil Temperature [C]	20
Fuel Injection Timing [CAD aTDC]	80
Fuel Injection Pressure [bar]	50

Table 2-2: Cold-idle operating conditions

The operating principle of SAI includes running the engine with an enriched mixture to provide combustible products in the exhaust. Late spark timing is used to increase exhaust temperature. High exhaust temperatures help to enhance oxidation reactions with the injected secondary air. In this study, four different combinations of engine enrichment and spark retardation were tested. These conditions were selected after reviewing a previous student's work regarding hydrocarbon emissions with SAI. Spark timings of 10 and 15 CAD aTDC were both tested at engine enrichment levels of engine lambda 0.8 and 0.9. This gave four engine condition combinations. For each of these test conditions, data were recorded without any secondary air to provide the baseline measures of exhaust products and particle concentrations. In subsequent tests, the fuel injection duration and throttle position were maintained the same as the baseline test, but secondary air was injected in varying amounts. In this way, the effects of varying SAI amounts could be quantified and compared to the baseline test. SAI

rates for all engine conditions were swept to produce lambda measurements in the exhaust of 0.95, 1.0, 1.05, 1.1, and 1.2.

As stated before, the use of the SMPS to measure particles required all tests to be performed under steady-state conditions. Engine operation was maintained constant and engine conditions were allowed to reach steady-state before measurement. This helped to ensure that particle production in the cylinders was steady for all tests at varying SAI rates. The other aspect deserving consideration was allowing the conditions in the exhaust system to reach steady-state before beginning the particle measurement. This was a more time consuming process for two reasons. First, exhaust stream temperatures were largely different for conditions with and without secondary air. Second, the exhaust system had a high thermal inertia, especially due to the presence of the turbocharger. It was observed in early tests that after SAI began, about fifteen minutes were required before the exhaust system and the exhaust stream temperatures reached steady-state. Due to the dependence of oxidation in the exhaust on the exhaust stream temperature, adequate time to achieve steady-state was an important consideration.

The SMPS system was setup for this study according to the operation manual [28]. This entailed selecting the correct flow rates of exhaust sample and excess air for the particle sizes and concentrations to be measured. The flow rate of nitrogen for diluting the sample was also closely regulated by a mass flow controller.

2.2.2 Data Collection

Data were collected for two main purposes. The first was to record data on the engine operation and the second was to record the particle measurements. Data from the engine was collected using a National Instruments data acquisition system (DAQ) and National Instruments LabView software. The data collected from the engine included, among additional things, cylinder pressure data, fluid temperatures, all pressure transducer data, engine speed and load, exhaust lambda, and exhaust system temperatures. The National Instruments DAQ also recorded the output of the NDIR exhaust analyzer. This provided undiluted measurements of CO and CO2 in the exhaust

gas. The engine data was collected for a period of 100 cycles. Data was taken at the beginning of each SMPS scan.

After the engine and exhaust temperatures reached steady-state, the measurements for a particular test could begin. For particle measurements this meant recording three scans of the particle spectrum. The particle spectrum was limited to particle sizes in the range of 23-350 nanometers. Each scan included an upward scan (60 seconds) and a downward scan (30 seconds). The particle measurements were acquired and recorded using the software provided by TSI with the SMPS. The total measurement process took 4.5 minutes. Engine data was collected at the beginning of each scan to record any potential changes in operation conditions over the 4.5 minute period. The additional Li-Cor NDIR CO2 analyzer was used to measure the CO2 concentration in the diluted exhaust sample that was fed into the SMPS. By comparing the CO2 concentration in the diluted sample to the CO2 concentration in the undiluted sample (from the Horiba NDIR), the nitrogen dilution ratio could be determined.

Exhaust wall temperatures were recorded in addition to the exhaust stream temperatures taken by thermocouples described in section 2.1.1. The temperature of the outer surface of the exhaust system at various locations was used to help quantify exhaust heat release. The method used for doing this is further described in section 2.3.2. Several attempts were made to attach surface measurement thermocouples to the exhaust system surface. This proved to be unsuccessful due to the failure of the high temperature cement to securely hold the thermocouple to the exhaust. Instead, a hand-held, infrared thermometer was used to measure the surface temperature at five locations along the exhaust system. These locations are shown on a diagram of the exhaust system in Figure 2-5. The measurements were manually recorded during testing. The exhaust system was marked at the location of the measurement to help ensure the temperature measurement was taken repeatedly at the same location.

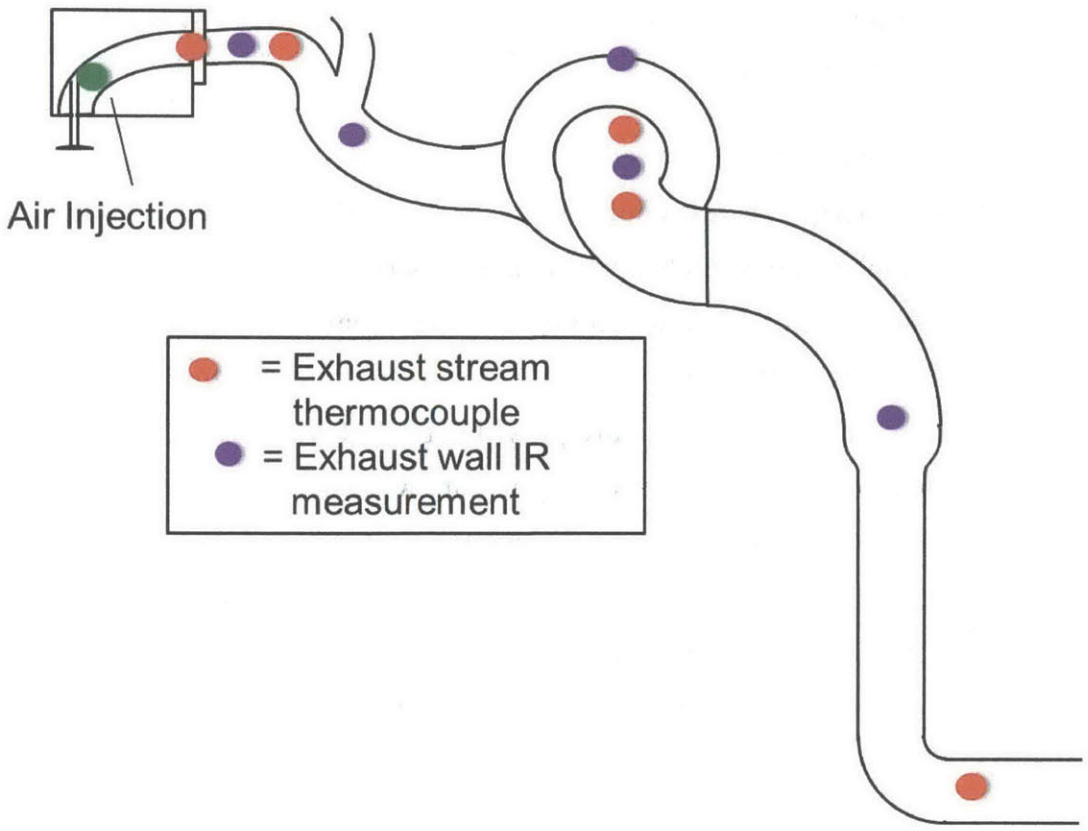

Figure 2-5: Exhaust thermocouple and surface temperature measurement locations

2.2.3 Data Processing

Post-processing of the engine data collected with National Instruments LabView software was accomplished using a Matlab program developed by a previous student. This program is described further in Kevin Cedrone's PhD thesis [29].

Much of the processing of the SMPS particle data was done by the TSI software. The recorded particle data could be exported in a variety of formats including particle distributions, cumulative particle number, and cumulative particle volume. All three forms of particle measurement are present in this work. Of note are the units of measurement for the particle distributions. The particle concentrations are measured for particular bins of particle sizes. Each bin represents a range of particle sizes. For the particle distribution plots, the particle concentration is normalized by the size of the

bin. This makes it possible to compare particle data from two different sampling instruments that may use different bin sizes. Additional information regarding the normalization and units for particle concentration are provided by TSI [30].

2.3 Analysis Methods

2.3.1 Particle Concentration Dilution Adjustment

It was necessary to dilute the exhaust sample with nitrogen so it could be accurately analyzed by the SMPS. This lowered the particle concentration in the sample to a level that would not saturate the SMPS. It also prevented nucleation of new particles by the condensation of volatile hydrocarbons as the sample cooled. The act of diluting the sample also made it necessary to adjust the measured particle concentrations. The actual concentration of particles in the exhaust was found by multiplying the measured concentration by the dilution ratio. As was discussed previously, the dilution ratio was given by the ratio of CO2 concentration in the undiluted and diluted exhaust samples. Adjusting for the dilution by nitrogen addition was a necessary part of analyzing the particle data.

The addition of secondary air diluted the exhaust flow in a similar fashion as the nitrogen dilution. Secondary air was introduced into the exhaust flow with the intention of providing the oxygen needed to oxidize the combustible products of the enriched fuel mixture. This additional air diluted the exhaust gas and effectively reduced the concentration of particulate matter. The intent of the tests was to measure the particle reduction from the baseline case, which used zero secondary air. For this reason, the particle concentrations for test cases with SAI were adjusted for the diluting effect of the additional air. The dilution ratio due to SAI was calculated using the equation below. The mass of fuel injected was constant for tests at given engine conditions, so the equation effectively gives the ratio of mass flow of air through the exhaust system. SAI dilution was most prominent for the cases with engine lambda of 0.8 and exhaust

lambda of 1.2. For those cases, the SAI dilution ratio was 1.46:1. The typical dilution ratio for nitrogen addition was 70:1.

$$SAI\ Dilution\ Ratio = \frac{\lambda_{Exhaust}(\frac{A}{F})_s + 1}{\lambda_{No\ SAI}(\frac{A}{F})_s + 1}$$

The density of the exhaust flow at the sampling location was another important consideration. Particle concentrations are measured as the number of particles in a given volume of exhaust gas. Therefore, as the density of the exhaust sample changes, so would the apparent concentration of particles. For instance, if a particular exhaust sample was heated, the density would decrease, the volume would increase, but the number of particles would remain the same. This would appear to cause a decrease in particle concentration. Exhaust temperatures at the sampling location varied greatly due to oxidation within the exhaust system under conditions for SAI. For this reason, the particle concentration measurements were normalized using a density normalization factor. The normalization factor was calculated with the equation below. The exhaust pressure and the temperature at the 'Post Turbo 3' thermocouple location were used to account for density changes due to differences in temperature or pressure. They were normalized to reference conditions of 300 K and 1 bar. This affected the absolute particle concentrations but enabled the comparison of relative particle reductions with SAI regardless of large temperature differences. The temperature measurement at the Post Turbo 3 location was used because it was located about 10 cm upstream of the sampling location.

$$Density\ Normalization\ Factor = \frac{T_{Post-Cat}}{300\ K}\frac{1\ bar}{P_{exhaust}}$$

2.3.2 Oxidation Estimate

Part of the intent of this study was to investigate the evolution of particles and the oxidation of combustible products with SAI. The particle reductions were measured

directly but other factors were not easily measured. The amount of heat released throughout the exhaust system could not be measured directly but could be estimated by analyzing the measured exhaust temperatures. Also, the location of heat release and particle oxidation in the exhaust system was of interest but also very difficult to measure directly. Instead, the available data for exhaust stream temperature, exhaust wall temperature, and exhaust gas composition were used to estimate the amount and location of heat release.

Quantifying the amount of enthalpy contained in the combustible exhaust products leaving the cylinder was important in determining heat release in the exhaust. The three main components of the exhaust that contributed to the chemical enthalpy in the mix were CO, H2, and hydrocarbons (HC). These were all present due to the enriched engine operation (lambda = 0.8 or 0.9). An equilibrium exhaust gas composition calculator written in Matlab was used to determine the levels of CO and H2 in the exhaust. Equilibrium calculations could not provide a reliable measure for HC, so instead a series of tests were performed. The tests included running the engine and using a Cambustion HFR-400 Fast FID to measure HC concentrations. This instrument measures HC concentrations by detecting ion production from the combustion of HC in an exhaust sample. A further description of the operation principle is available from Cambustion [31]. The tests were conducted with the same operating conditions as the particle measurement tests. The replicated conditions included the thermal conditions, engine speed, engine load, and spark timing (both 10 and 15 CAD aTDC). Tests were conducted at engine enrichment levels of both lambda 0.8 and 0.9, in addition to several other intermediate enrichment levels. This enabled general trends to be observed and for the HC concentrations to be quantified. The resulting plot is below.

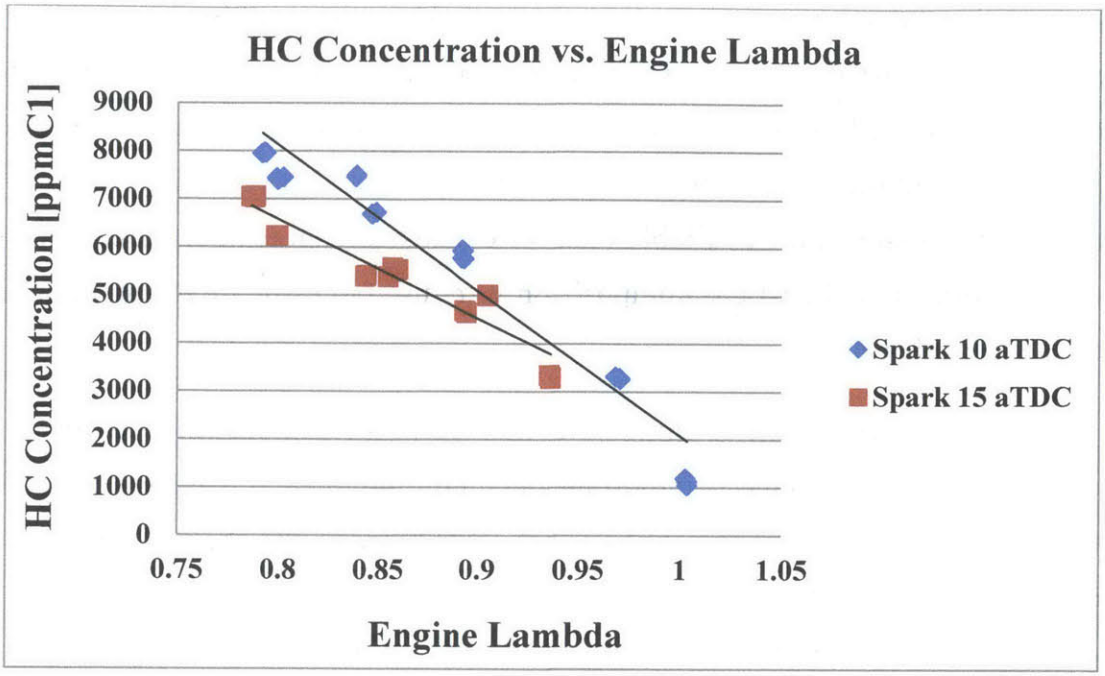

Figure 2-6: Exhaust hydrocarbon concentration for particle measurement tests

The results of the hydrocarbon measurements and the equilibrium calculation were used to estimate the chemical enthalpy content of the exhaust flow for the tests including SAI. The table below specifies the total chemical enthalpy of the exhaust flow and the percentage contributions of CO, H2, and HC for the specified engine operation conditions.

Engine Lambda	Spark Timing [aTDC]	Exhaust Enthalpy [kJ/kg exhaust]	Percent Enthalpy Contribution		
			CO	H2	HC
0.9	10	520	63%	16%	21%
0.9	15	510	64%	17%	19%
0.8	10	1070	65%	20%	15%
0.8	15	1050	66%	21%	14%

Table 2-3: Exhaust chemical enthalpy summary

It was found that the chemical enthalpy in the exhaust flow was primarily due to the presence of CO for all tests. CO was also easily measured using the Horiba NDIR. For these reasons, CO was used as an indicator of overall chemical enthalpy in the exhaust. Therefore, the measured reduction of CO could estimate the overall fraction of chemical enthalpy released in the exhaust system. In tests with secondary air, the CO concentrations were adjusted for the dilution effect of SAI before they were used to determine oxidation amounts. The term 'Oxidation Percent' will be used in this study and it represents the portion of the exhaust chemical enthalpy that was released by oxidation within the exhaust system. It was calculated as the percent reduction of CO concentration in the SAI tests as compared to the baseline test without SAI. The equation used is shown below.

$$CO\ Reduction = 100\% * \left(1 - \frac{x_{CO;\ with\ SAI}}{x_{CO;\ zero\ SAI}}\right)$$

The total fraction of available chemical enthalpy as represented by the oxidation percent was a useful way to measure the effectiveness of SAI in different flow rates and at different engine conditions. It was further desired to investigate the location within the exhaust system that oxidation was occurring. To achieve this, the exhaust system was outfitted with five thermocouples and five measurements of the exhaust system outer wall were taken manually during every test. These temperature measurements were used to perform an energy balance on four discrete zones in the exhaust system. Each of these zones was defined by a portion of exhaust system where there was a thermocouple available to measure the exhaust gas temperature at the entry and exit of the zone. The presence of five exhaust gas thermocouples therefore allowed the energy balance to be performed on four zones in the exhaust. These were numbered one through four. A fifth zone, Zone 0, was determined to be the portion of the exhaust system upstream of the first thermocouple location. This zone consisted of mainly the exhaust port and only a small section of exhaust manifold runner. The lack of a thermocouple measurement of exhaust temperature at the entry of the zone eliminated the ability to perform an energy balance on Zone 0. Instead, the portion of oxidation

that occurred in Zone 0 was defined to be the total oxidation percent as calculated using CO reduction, minus the total oxidation of Zones 1-4 as calculated using an energy balance. The location of the zones, exhaust gas thermocouples, and exhaust surface measurement locations are shown in Figure 2-7, below.

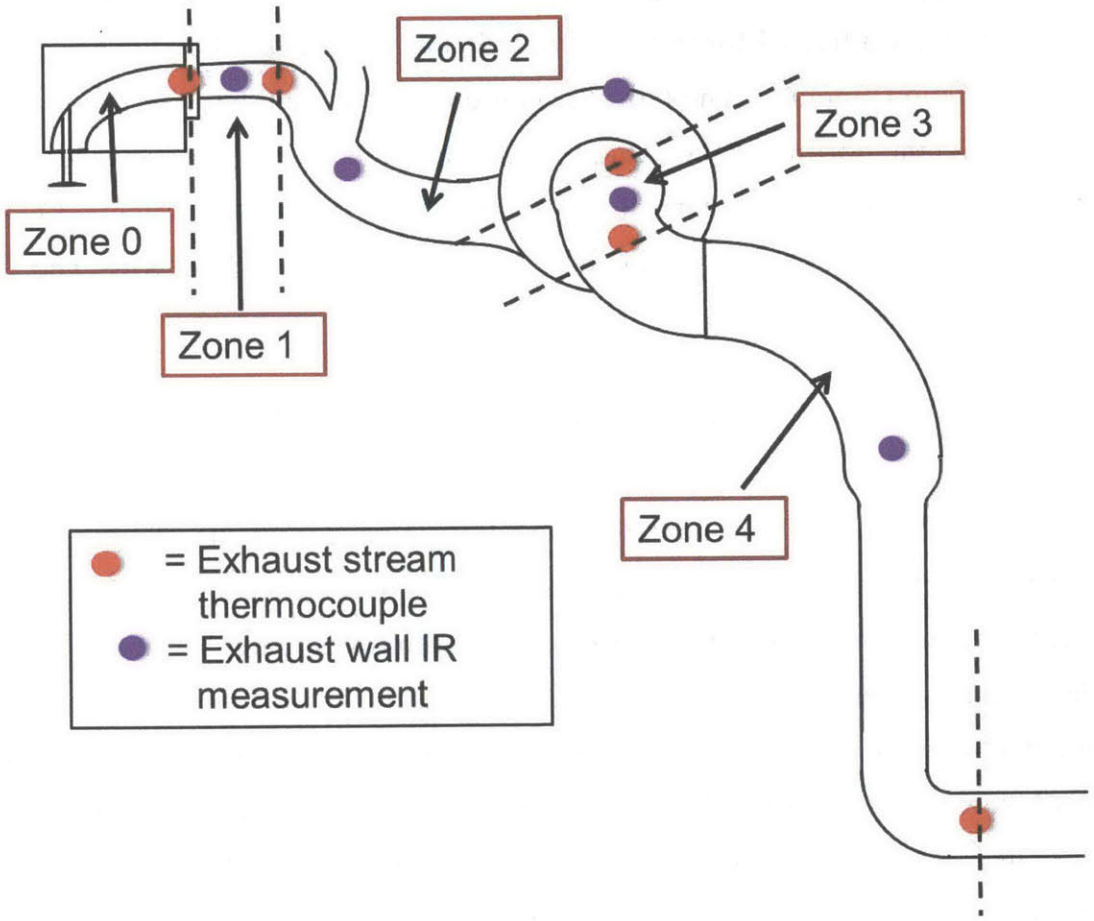

Figure 2-7: Oxidation analysis exhaust zone locations

For analysis purposes, a control volume was drawn around each of the four zones. A diagram of the control volume is shown in Figure 2-8. The diagram shows energy flows into and out of the control volume due to the flow of hot exhaust gases through the zone. $\dot{Q}_{LOSS}$ is the term that represents the rate of heat energy lost to the ambient through the walls of the zone. The rate of energy generation in the zone by the release of chemical enthalpy is represented by $\dot{Q}_{GEN}$.

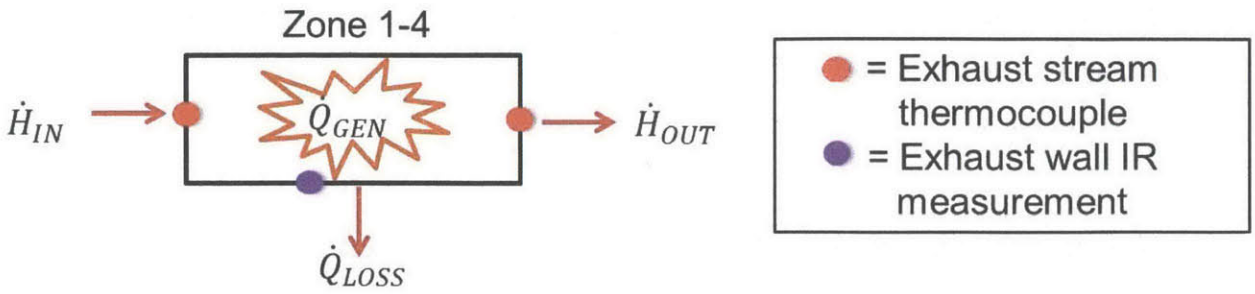

Figure 2-8: Control volume for oxidation estimate in Zones 1-4

The energy balance equation for the various heat flows is below. $\dot{Q}_{GEN}$ is the value of interest because it gives the amount of heat that was produced by oxidizing exhaust products within the zone.

$$\dot{Q}_{GEN} = \dot{Q}_{LOSS} + \dot{H}_{OUT} - \dot{H}_{IN}$$

$\dot{H}_{IN}$ and $\dot{H}_{OUT}$ are the enthalpy flows in and out of the control volume. The values for these terms are given by the expressions below. $\dot{Q}_{LOSS}$ is estimated by using the convective heat transfer coefficient (h), the area of the exposed section of exhaust system wall (A), and the difference in temperature of the exhaust gas and the wall. The gas temperature was taken to be the average reading from the thermocouple at the entrance and exit of the zone (T_{AVG}). The inner wall temperature (T_{WALL}) was assumed to be equal to the outer wall temperature that was measured using an IR thermometer. This was valid because the temperature difference between the inner and outer wall surfaces was much smaller than the difference between the gas temperature and the wall temperature.

$$\dot{Q}_{LOSS} = h\,A(T_{AVG} - T_{WALL})$$

The energy flows into and out of the zone due to the flow of exhaust gas are given by the specific heat of the exhaust gas and the gas temperature. The specific heat (C_p) was calculated as a mass weighted average of the specific heat of stoichiometric exhaust products [9] and excess air due to SAI. The temperature of gases entering the

zone (T_{IN}) and exiting the zone (T_{OUT}) were given by the exhaust gas thermocouples at the boundaries of each zone.

$$\dot{H}_{IN} - \dot{H}_{OUT} = \dot{m}_{EXH} C_p (T_{IN} - T_{OUT})$$

The expressions above can be used to find $\dot{Q}_{GEN}$ by inputting the measured temperatures into the given equations. For the purposes of this study it was most useful to express the heat released in each zone as a fractional portion of the total chemical enthalpy contained in the exhaust products ($\dot{Q}_{CHEM}$). This is shown in the equation below. Values for $q_{CHEM}\left[\frac{kJ}{kg}\right]$ for the required engine operating conditions are given in Table 2-3.

$$Fraction\ of\ heat\ release\ per\ zone = \frac{\dot{Q}_{GEN}}{\dot{Q}_{CHEM}} = \frac{hA(T_{AVG} - T_{WALL}) - \dot{m}_{EXH} C_p (T_{IN} - T_{OUT})}{\dot{m}_{EXH} q_{CHEM}}$$

A value for the collective term for convective heat transfer coefficient and wall surface area (hA) was needed to use the equation above. This term could be calibrated from the data for baseline tests without SAI. In these tests no secondary air was used so the chemical heat release ($\dot{Q}_{GEN}$) in each zone was zero. This allowed for the simplified equation shown below. The equation enabled the calculation of (hA) for each zone by using the measured temperatures from the baseline, zero SAI tests.

$$\dot{Q}_{LOSS} = E_{IN} - E_{OUT}$$

$$hA = \frac{\dot{m}_{EXH} C_p (T_{IN} - T_{OUT})}{(T_{AVG} - T_{WALL})}$$

With the above equations, the oxidation estimate could be performed. The results of this estimate gave the amount of heat released in each zone as a fraction of the engine-out chemical enthalpy. For Zones 1-4, fraction of heat released was estimated using an energy balance. As discussed earlier in this section, the total fraction of exhaust chemical enthalpy that was released was estimated by the reduction of CO concentration. This procedure implies that the extent of HC and H2 oxidation are the

same as that of CO. An estimate for the heat released in Zone 0 was made by subtracting the sum of the heat release fractions for Zones 1-4 from the total heat release. The method outlined in this section helped to identify where in the exhaust system the bulk of the oxidation of exhaust products occurred. The results of this analysis will be discussed in depth later in this study.

Chapter 3: Experimental Results

The experiments performed in this study have been outlined in previous sections. The results of the experiments will be presented here. Results are presented in three main sections: exhaust stream temperature analysis, oxidation analysis, and particle emissions effects.

3.1 Exhaust Stream Temperature

Analysis of the exhaust stream temperature was an important step in determining the effects of SAI on processes occurring in the exhaust system. The temperatures were measured by k-type thermocouples at five locations throughout the exhaust stream. The locations of these measurements are illustrated in Figure 2-1and Figure 2-5. The temperatures measured at these locations were used to determine the temperature increases associated with SAI oxidation. The temperatures were also instrumental in performing the oxidation estimate, the results of which will be presented in a following section. The results of the temperature measurement and oxidation analysis quantified the amount and location of oxidation due to SAI within the exhaust system.

The temperature measurements are presented in four plots, one for each engine operating condition. These conditions included spark timings of 10 and 15 degrees aTDC at each of the two enrichment levels. The engine enrichment levels were engine lambda of 0.8 and 0.9. At each of these engine conditions, a baseline test was performed for which no secondary air was injected. This allowed for baseline exhaust stream temperatures to be established. These tests also gave the baseline engine-out PM emissions for each operating condition. For the subsequent tests, SAI was used in increasing amounts to produce exhaust lambda values of 0.95, 1.0, 1.05, 1.1, and 1.2. The following plots illustrate the temperature at the five thermocouple locations for the baseline (no SAI) and each of the five SAI rates.

3.1.1 Engine Lambda = 0.9, Spark Timing = 10 aTDC

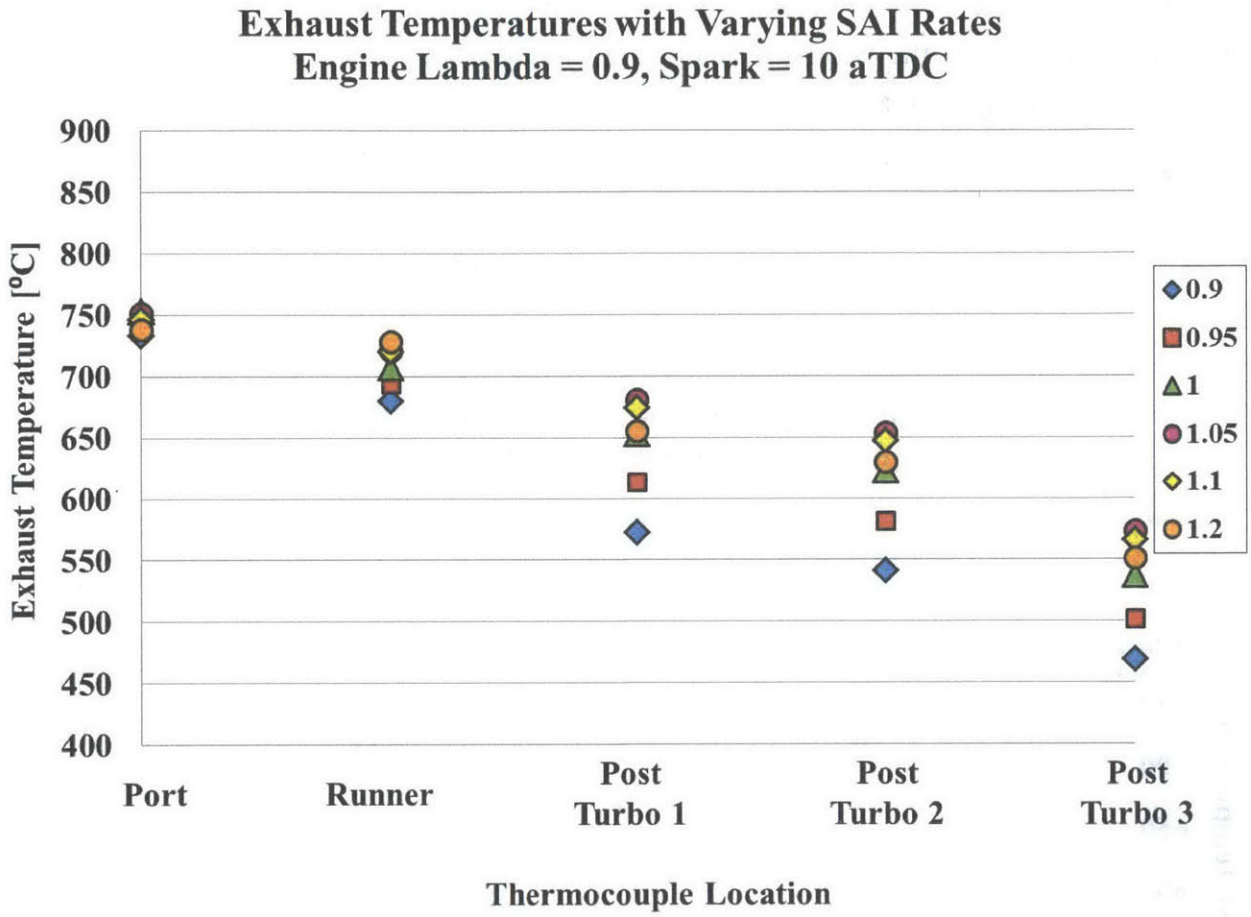

Figure 3-1: Exhaust stream temperature: Engine lambda=0.9, Spark=10 aTDC

The results for the spark=10, engine lambda=0.9 tests gave the lowest temperatures for any of the tested engine conditions. This was a result of it being the earliest spark timing and the highest engine lambda. The less enriched engine mixture produced a lower concentration of combustible exhaust products. Therefore, there was reduced enthalpy release in the exhaust. The results did show evidence of measureable oxidation in the exhaust by the increase in exhaust stream temperature. This increase in exhaust stream temperature was seen at all SAI rates. Temperatures were highest at the port thermocouple and then decreased along the length of the exhaust system due to

heat loss. In cases with SAI, a portion of this heat loss was offset by the heat released from oxidizing exhaust products. The highest temperature increases were observed at the three downstream thermocouple locations (Post Turbo 1, Post Turbo 2, Post Turbo 3). At these locations, the largest temperature increases vs. the baseline case occurred with exhaust lambda = 1.05.

3.1.2 Engine Lambda = 0.9, Spark Timing = 15 aTDC

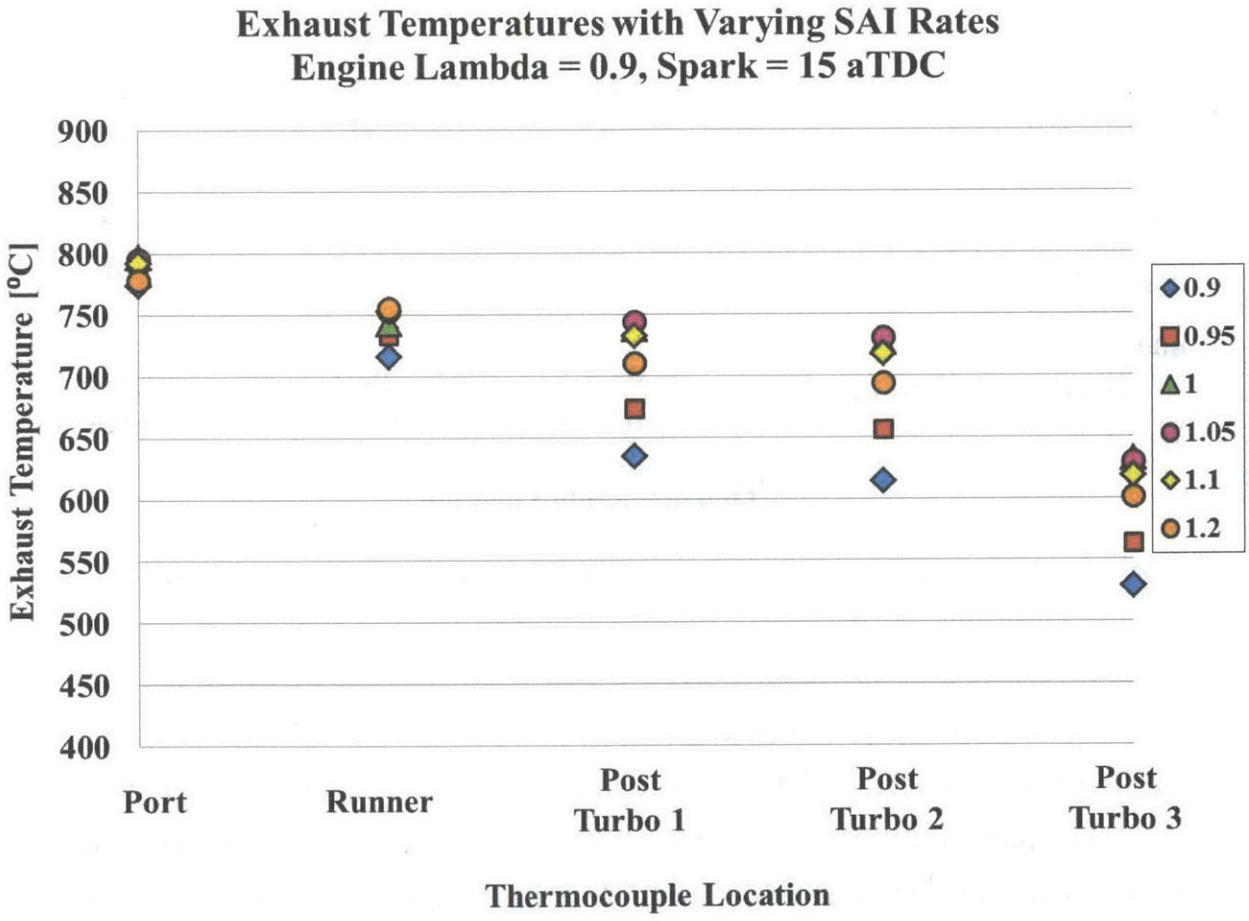

Figure 3-2: Exhaust stream temperature: Engine lambda=0.9, Spark=15 aTDC

The second engine condition retained the same enrichment level of engine lambda = 0.9, but spark timing was retarded to 15 degrees aTDC. It was expected that this case would produce higher temperatures due to the higher cylinder-out temperatures with later spark timing. The measured temperatures supported this and a typical increase of 50 °C was observed at the port thermocouple for all SAI rates. The temperatures in this case were also highest at the exhaust port and decreased downstream. Increased temperatures as compared to the spark timing = 10 case were apparent throughout the exhaust system. These increases were larger at the downstream locations. At the three downstream locations, peak temperatures for the later spark tests were about 65 °C higher than the peak temperatures in the earlier spark tests. At the port, the difference was about 50°C. This suggested that the higher temperature increases weren't only due to later spark, but were also a result of more complete oxidation. Similar to the earlier spark case, the highest temperature increases over the baseline test were again observed for the exhaust lambda = 1.05 case.

3.1.3 Engine Lambda = 0.8, Spark Timing = 10 aTDC

The second group of engine conditions tested utilized a higher enrichment level of engine lambda = 0.8. In these tests, there was a higher concentration of combustible products and more than double the exhaust enthalpy content as compared to the 0.9 tests. A summary of exhaust chemical enthalpy for the four test conditions is provided in Table 2-3. Much higher temperatures were observed in this test as compared to the tests at engine lambda = 0.9. This is with the exception of the Port thermocouple location. The higher enrichment level reduced the portion of fuel energy that could be released within the cylinder due to insufficient oxygen. Port thermocouple temperatures in this test were the lowest of any of the tested engine conditions. The effects of the lower cylinder-out temperature were negated by the higher energy release within the exhaust. Temperatures for the cases with SAI peaked at the Post Turbo 1 location and were typically 50-75°C higher than at the Port location. Very large temperature increases compared to the baseline were seen at the three downstream locations for all

SAI rates. The increases were highest at the Post Turbo 2 location for exhaust lambda of 1.0 and 1.05. These tests gave a temperature increase of about 270°C. The very high temperature increases with SAI as compared to the baseline indicate a high amount of energy release within the exhaust system from the oxidation of exhaust products.

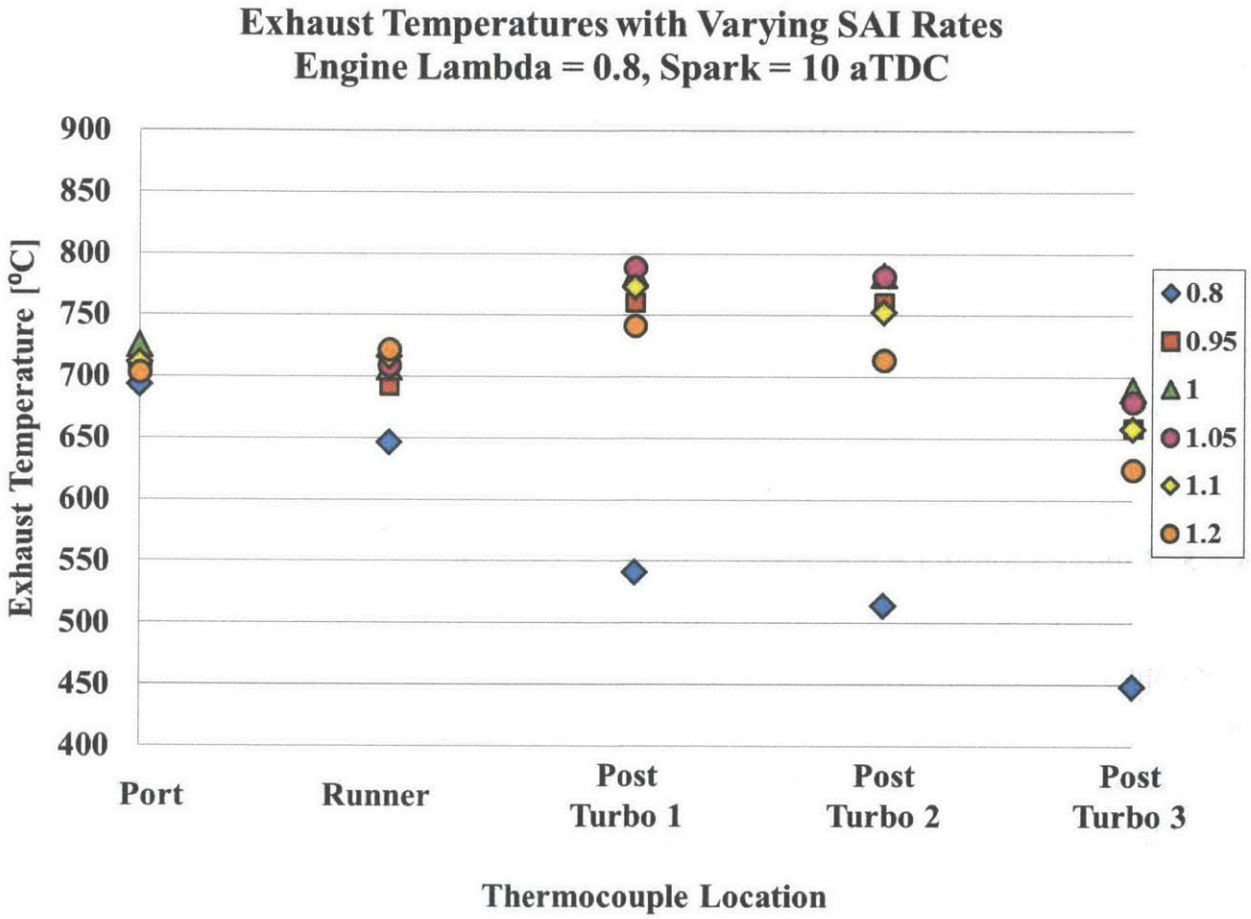

Figure 3-3: Exhaust stream temperature: Engine lambda=0.8, Spark=10 aTDC

3.1.4 Engine Lambda = 0.8, Spark Timing = 15 aTDC

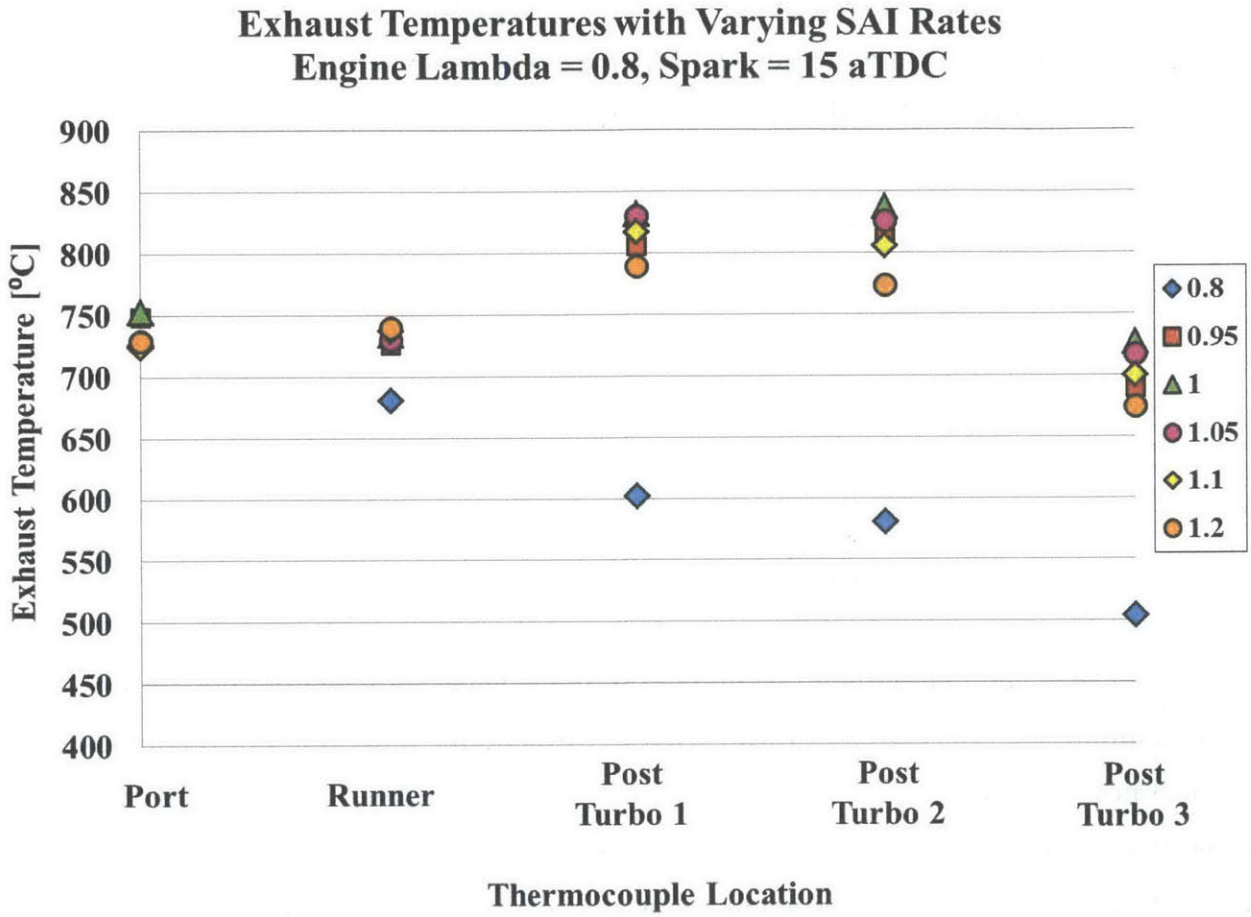

Figure 3-4: Exhaust stream temperature: Engine lambda=0.8, Spark=15 aTDC

The final set of engine conditions that were tested were at an engine lambda of 0.8 and a spark timing of 15 aTDC. Perhaps unsurprisingly, this test produced the highest recorded temperatures among all the engine conditions that were tested. Temperatures at the Port thermocouple location were lower than those for the engine lambda = 0.9 test with the same spark timing. This again is attributed to less heat release within the cylinder due to insufficient oxygen. As with the other engine lambda = 0.8 test, large temperature increases were achieved with SAI in all amounts at the Post Turbo 1, Post Turbo 2, and Post Turbo 3 thermocouple locations. For these

locations, the exhaust temperature was at least 210°C higher than the baseline with exhaust lambdas of 1.0 and 1.05. The maximum exhaust temperature increase was 260°C at the Post Turbo 2 location and an exhaust lambda of 1.0. Peak temperatures at each location were typically achieved with an exhaust lambda of 1.0. Although, exhaust lambda of 1.05 produced similar peak temperatures.

3.2 Oxidation Analysis

The exhaust stream temperature measurements offered some insight into the effectiveness of SAI and the oxidation of combustible exhaust products. It was still desired to estimate the amount of heat released within the exhaust system. Furthermore, it was useful to know the location within the exhaust system where oxidation was occurring. To achieve these goals, an oxidation analysis was performed. This included estimating the chemical enthalpy contained in the exhaust flow leaving the cylinder. Carbon monoxide (CO) reduction was used to estimate the reduction of all combustible exhaust products. This gave an estimate of total chemical enthalpy released within the exhaust system. Finally, an energy balance was performed on discrete zones of the exhaust system. Together, these methods produced an estimate of the amount of heat released in five zones within the exhaust system. A more thorough description of the oxidation analysis has been provided in section 2.3.2

3.2.1 Total Oxidation Estimate

The total amount of oxidation that occurred in the exhaust system was estimated by calculating the reduction of CO. This analysis assumes that hydrogen and hydrocarbon exhaust concentrations are reduced in the same proportion as CO. CO contributed about two-thirds of the exhaust chemical enthalpy. A summary of the CO reduction as a percentage for all tests is presented in Table 3-1.

CO Reduction [%]						
		Exhaust Lambda				
Engine Lambda	Spark Timing [deg aTDC]	0.95	1	1.05	1.1	1.2
0.9	10	17.2	44.8	75.3	81.0	84.6
0.9	15	21.5	79.2	96.4	95.9	94.7
0.8	10	74.4	98.5	99.4	98.0	93.5
0.8	15	75.4	97.1	99.8	99.6	98.5

Table 3-1: CO reduction percent for all tests

3.2.2 Cumulative Oxidation: Engine Lambda=0.9, Spark=10 aTDC

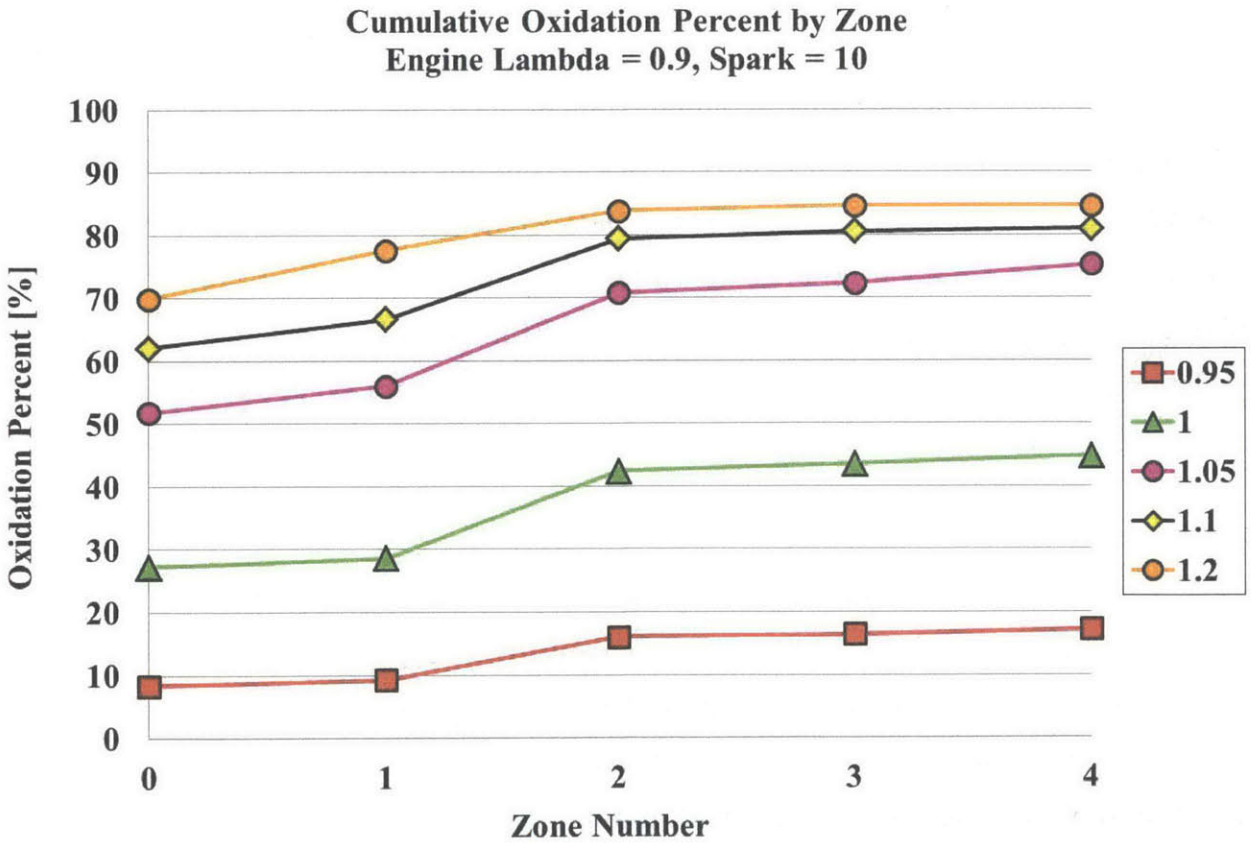

Figure 3-5: Cumulative oxidation by zone for engine lambda=0.9, spark=10aTDC

The first engine conditions that were tested included an engine enrichment level of lambda = 0.9 and a spark timing of 10 degrees aTDC. As seen in the exhaust stream analysis, these conditions yielded the lowest exhaust temperatures. Table 3-1also shows that these conditions gave the lowest total CO reduction (oxidation percent). The above plot offers some insight into why total CO reduction may have been lowest for these conditions. As seen in this plot, and the plots that will follow, only a small portion of the total oxidation occurred in Zones 3 or 4. The most significant oxidation took place in Zone 0 for all tests. This is due to the conditions required for robust oxidation with SAI. Combustible exhaust products, temperatures high enough to initiate oxidation, and fast entrainment of oxygen from secondary air are all important for SAI oxidation. Fast mixing of exhaust products and secondary air is necessary to provide sufficient oxygen to the reaction before too much heat is lost to the exhaust system. If excessive heat loss occurs, temperatures become too low to initiate the reaction. The engine conditions in this test were at the lower of the two enrichment levels and the earlier of the two spark timings. The lower concentration of combustible products and the lower engine out temperatures increased the significance of fast mixing for robust oxidation. The data shows that oxidation in Zone 0 increased as the secondary air rate increased. This was an effect of having more air in the exhaust port at blowdown and therefore faster mixing of exhaust and secondary air. It was also estimated that only a small portion of oxidation occurred in Zones 1-4. Therefore, the trends seen for Zone 0 reflected the trends seen for total CO reduction.

3.2.3 Cumulative Oxidation: Engine Lambda=0.9, Spark=15 aTDC

The second set of engine conditions tested were for engine lambda = 0.9 and spark timing = 15 degrees aTDC. These conditions provided approximately the same concentration of combustible exhaust products as the previous case, but the exhaust temperature was higher due to later spark timing. This helped to initiate oxidation within the exhaust port and the effects are reflected in the oxidation data. Table 3-1shows large increases in CO reduction for all secondary air rates as compared to the previous engine condition. For the three highest air rates, CO reduction was about 95%.

Oxidation within Zone 0 again constituted a large majority of the total oxidation. Zone 0 oxidation amounts were observed to increase as the secondary air rate increased. This was due to the effect of better mixing within the exhaust port when a higher amount of secondary air was being injected. For the three highest secondary air rates (exhaust lambda = 1.05, 1.1, and 1.2), the total CO reduction was quite similar. These tests showed a trend of increasing Zone 0 oxidation with increasing air rate. The remaining oxidation was primarily accounted for in Zone 2. In Zone 2, exhaust lambda = 1.05 yielded the highest oxidation amount and oxidation decreased with increasing air rate. These air rates all yielded a high overall CO reduction, but oxidation occurred further downstream as air rate decreased. This was again an effect of faster mixing within the exhaust port as air rate increased. This caused a higher portion of the total oxidation to occur further upstream.

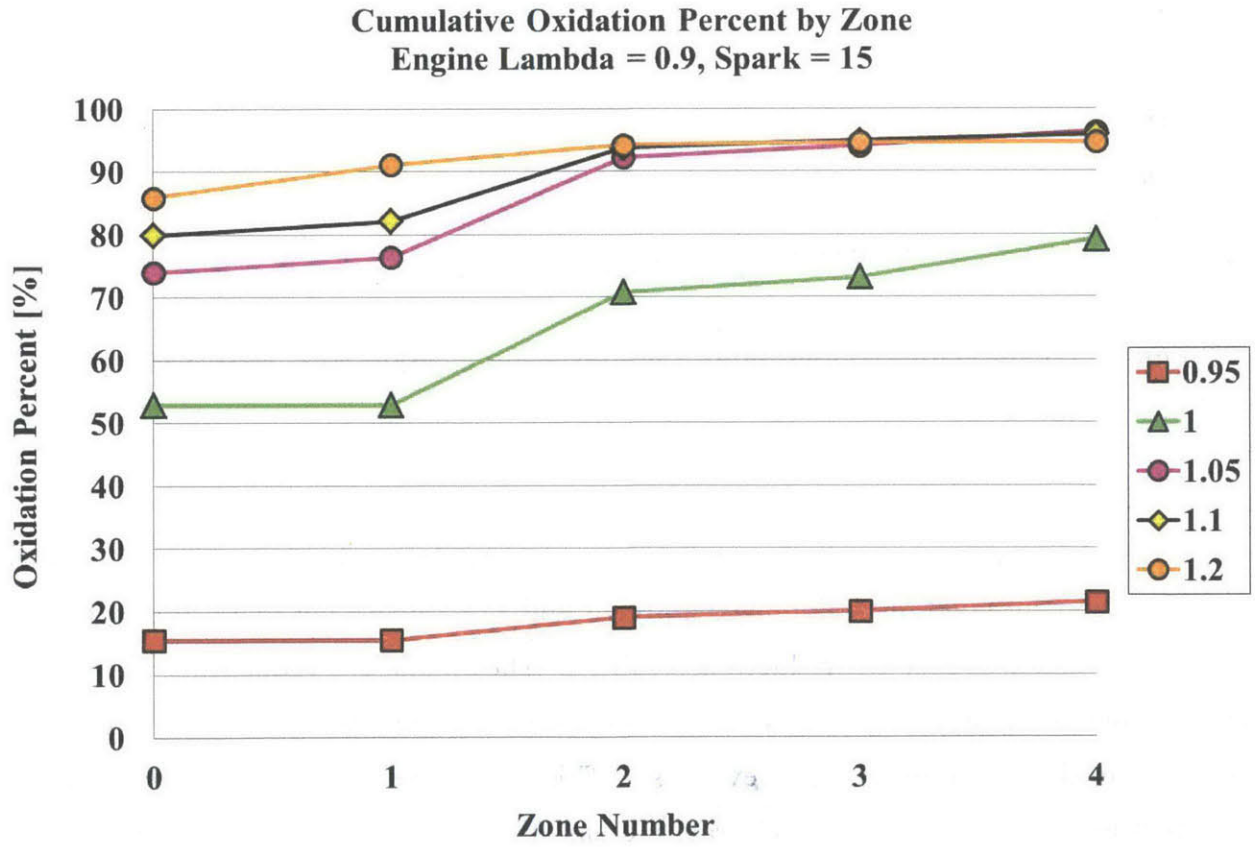

Figure 3-6: Cumulative oxidation by zone for engine lambda=0.9, spark=15 aTDC

3.2.4 Cumulative Oxidation: Exhaust Lambda=0.8, Spark=10

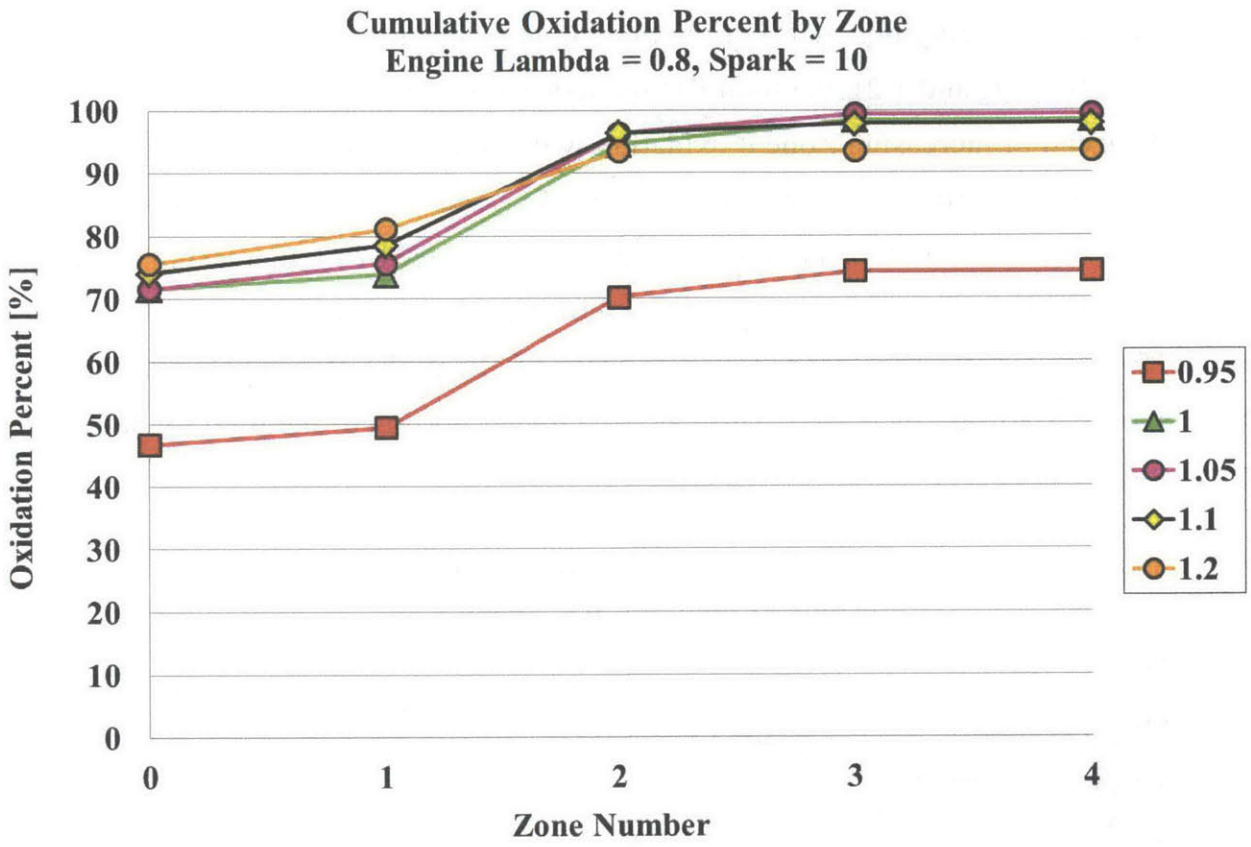

Figure 3-7: Cumulative oxidation by zone for engine lambda=0.8, spark=10 aTDC

In this test, the engine enrichment level was lambda = 0.8. This yielded about twice the exhaust chemical enthalpy as for the engine lambda = 0.9 tests. Therefore, the higher enrichment level tests displayed a higher enthalpy release per mass of exhaust, which led to much higher CO reductions. Table 3-1shows that CO reductions were typically much higher at a given exhaust lambda for the higher enrichment level tests as compared to the lower enrichment level tests. This test showed the usual trend that the oxidation in Zone 0 increased as SAI rate increased. This was due to the faster mixing in the exhaust port for tests with higher air rates. An interesting result from this engine condition was that CO reduction peaked for exhaust lambda = 1.05 and declined for the

higher secondary air rates. This was caused by the excess air that did not participate in the reaction but acted as a diluent in the exhaust. This creates a trade-off between using higher air rates to achieve fast mixing in the port or staying closer to stoichiometric exhaust mixtures to limit the dilution effect. This trade-off has been previously noted by Hernandez et al. [32]. For the cases near stoichiometric (exhaust lambda = 1.0 and 1.05), a high overall CO reduction was still achieved, but the oxidation occurred further downstream than for exhaust lambda = 1.1 and 1.2. This is illustrated by the oxidation amounts in Zone 2 for these tests.

3.2.5 Cumulative Oxidation: Engine Lambda=0.8, Spark=15 aTDC

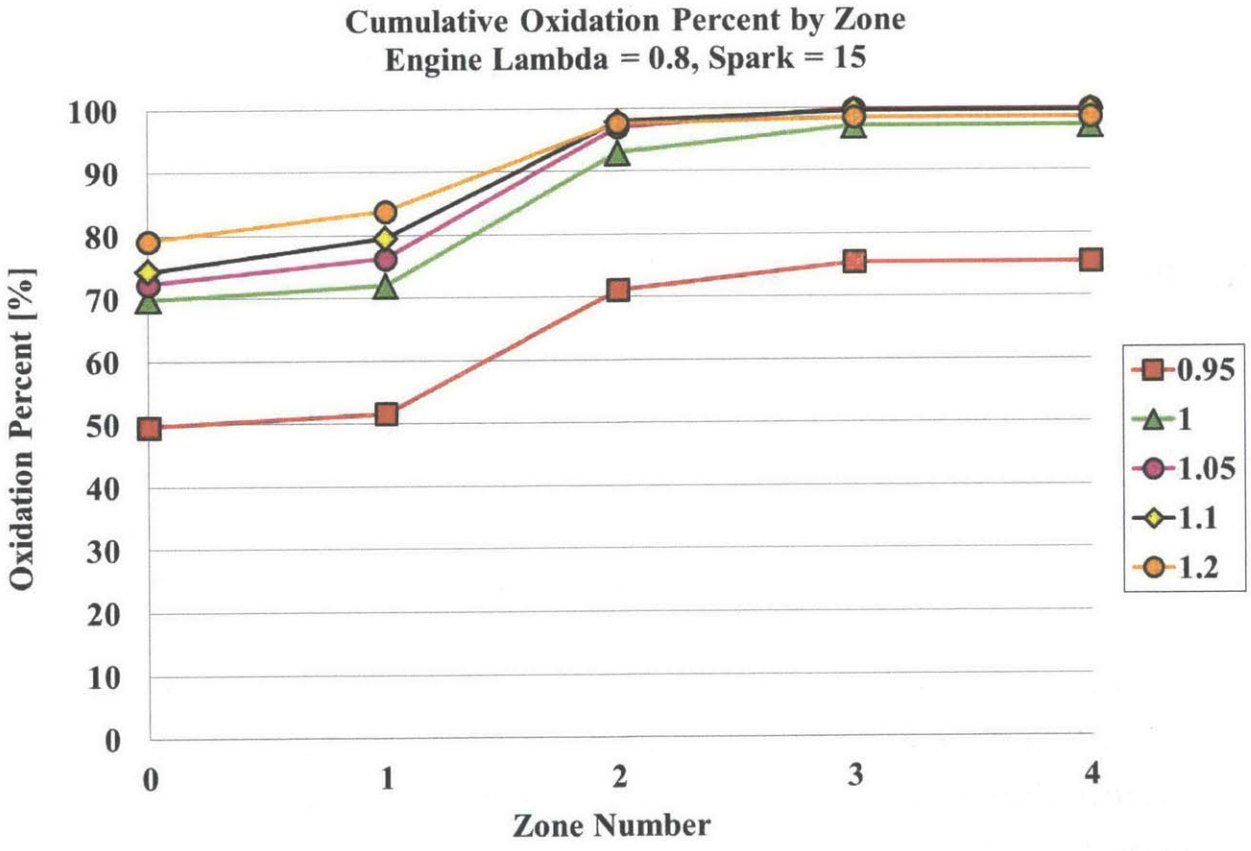

Figure 3-8: Cumulative oxidation by zone for engine lambda=0.8, spark=15 aTDC

It was expected that the final engine conditions tested would produce the highest total CO reductions. This case was run with engine lambda = 0.8 and spark timing = 15 degrees aTDC. The temperature data showed that these engine conditions yielded the highest exhaust stream temperatures. It is seen in Table 3-1that this test typically produced the highest CO reduction for a given exhaust lambda. Exhaust oxidation was most complete at this engine condition because of the high concentration of combustible products and the late spark timing. The trends seen in this test are very similar to those observed in the previous test. Oxidation in Zone 0 represented the majority of the total oxidation. Zone 0 oxidation increased as the SAI rate increased. Also, similar to the previous test, total CO reduction peaked for exhaust lambda = 1.05 and then decreased as SAI rate was increased. Total oxidation for the tests with exhaust lambda = 1.0 or higher were all quite similar. It is seen that as SAI rate increased, oxidation occurred further upstream. This was also observed in the previous test. The effects of faster exhaust port mixing and increased dilution from excess air with higher air rates were similar for both engine lambda = 0.8 tests.

3.3 Particulate Matter Emissions

The focus of this study was to investigate the effects of secondary air injection on particulate matter emissions. This section will present the PM emissions test results. The results will first be presented as particle distributions. The distribution plots illustrate the particle concentrations as a function of particle size. The plot lines are labeled according to their respective exhaust lambda. The 0.8 and 0.9 lines represent the engine out PM emissions for the cases without SAI. All of the particle measurements have been adjusted for the dilution effect of SAI. This is further detailed in section 2.3.1. Particle distributions are presented for each of the four engine running conditions. Later plots will show total particle number concentration and total particle volume concentration.

3.3.1 Particle Distribution: Engine Lambda=0.9, Spark=10 aTDC

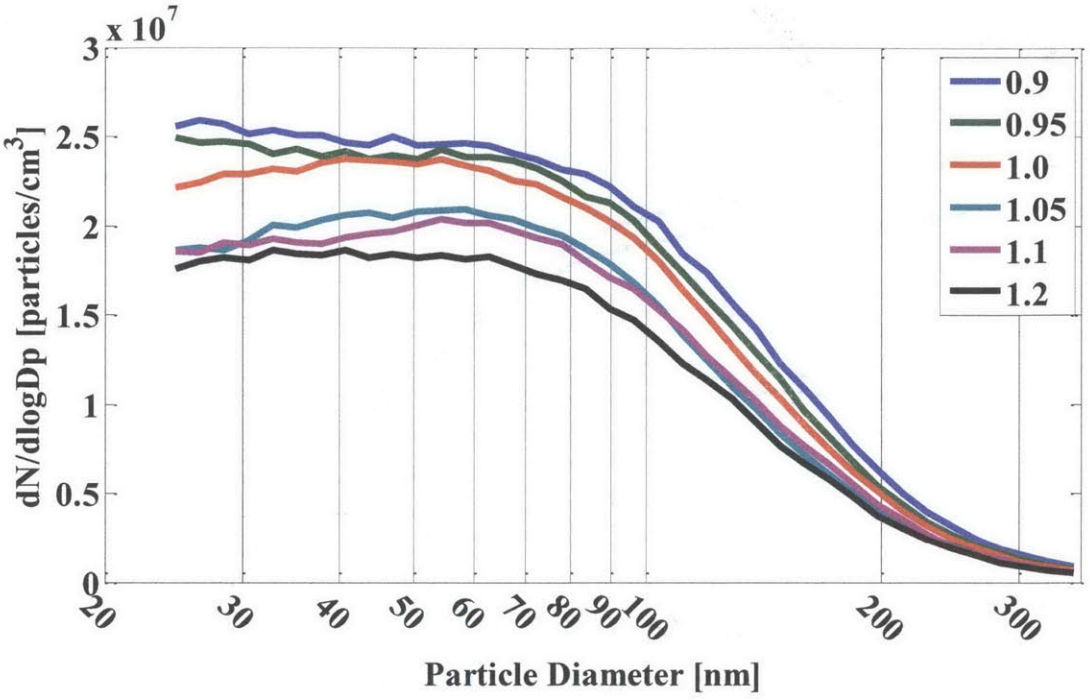

Figure 3-9: Particle distribution for engine lambda=0.9, spark=10 aTDC

The particle distribution for engine lambda = 0.9 and spark timing = 10 degrees aTDC is shown in Figure 3-9. It clearly shows that particle emissions were reduced across the entire spectrum for all secondary air rates. PM emissions decreased as SAI rate increased. The reductions were largest for particles in the range of 23-100 nm and reductions decreased at larger particle sizes. The particle distributions retain their shape for the various SAI rates but are flattened slightly as the particle concentrations decrease. The lowest PM emissions were observed for the test with exhaust lambda = 1.2.

3.3.2 Particle Distribution: Engine Lambda=0.9, Spark=15 aTDC

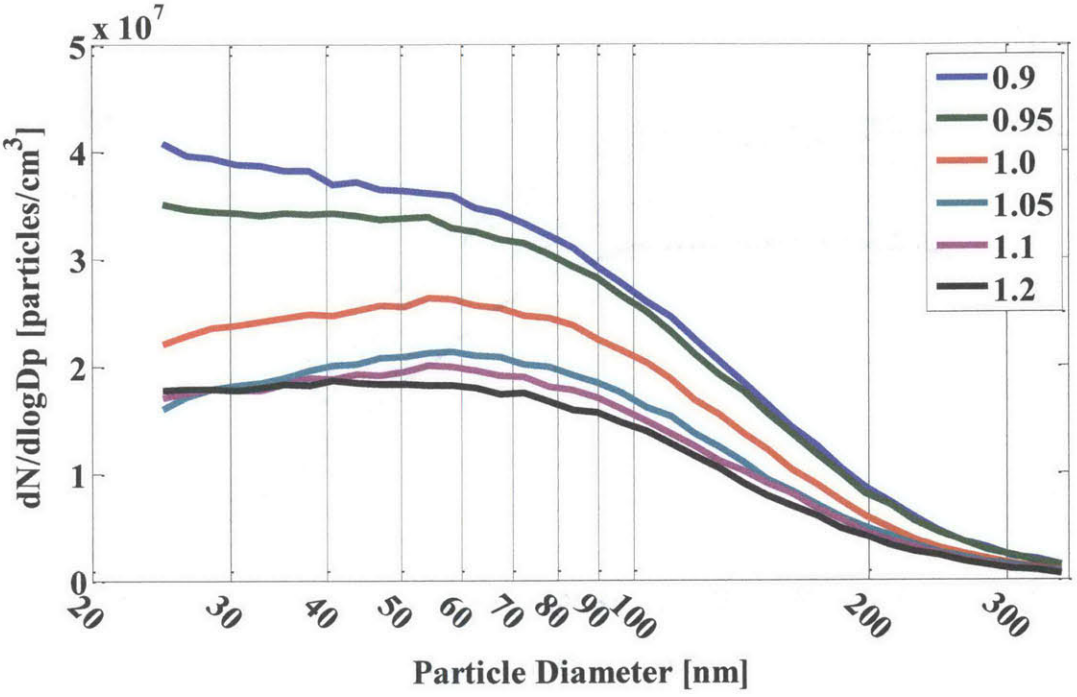

Figure 3-10: Particle distribution for engine lambda=0.9, spark=15 aTDC

In the second test, engine enrichment level stayed at engine lambda = 0.9, but spark timing was retarded to 15 degrees aTDC. The same basic trends are seen in this test as for the previous test. Particle concentrations for all particle sizes are reduced as SAI rate increases. Particle reductions are larger at smaller particle sizes and generally decrease as particle size increases. The basic distribution shape is the same for all exhaust lambda test, but is slightly flattened at higher SAI rates. There is a noticeable difference in baseline (no SAI) particle distributions between this test and the previous one. The shape of the baseline distributions look quite similar but particle concentrations for the later spark timing test are about 1.5 times greater than for the earlier spark timing. This is likely due to the effects of spark timing on PM formation as was discussed in the introduction. As combustion quality deteriorates with retarding spark, PM emissions are expected to increase. The lowest particle distribution was achieved with exhaust lambda = 1.2 for both cases. The traces corresponding to the

lowest PM emissions look quite similar in both shape and concentration level for both engine conditions.

3.3.3 Particle Distribution: Engine Lambda=0.8, Spark=10 aTDC

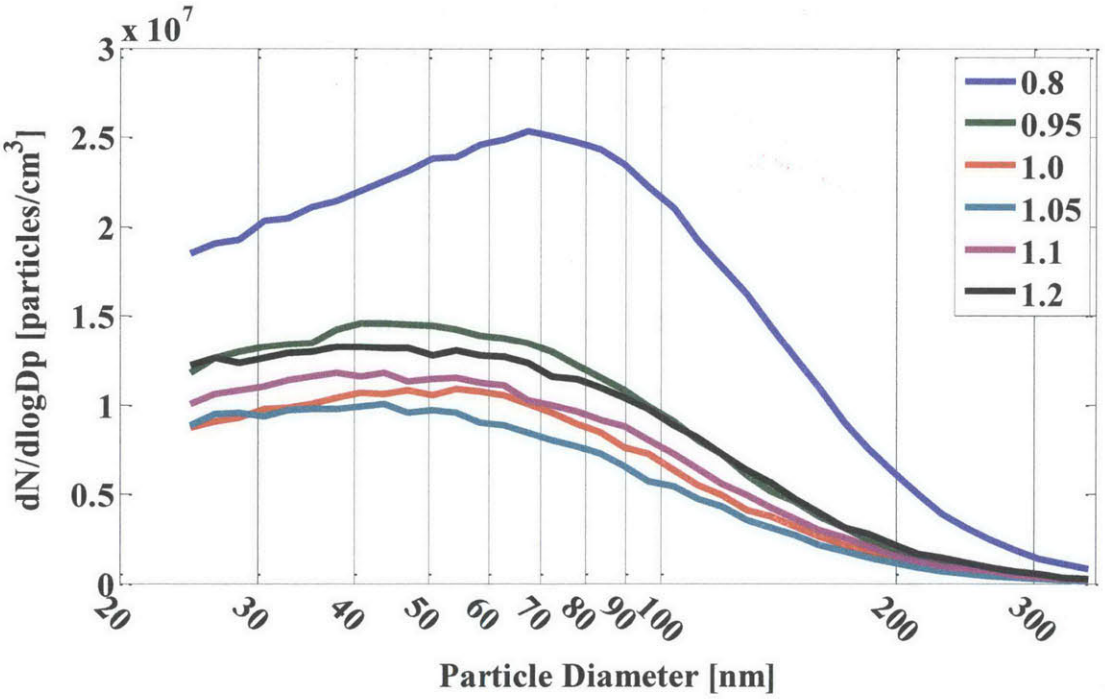

Figure 3-11: Particle distribution for engine lambda=0.8, spark=10 aTDC

Large particle reductions were also achieved in the higher engine enrichment tests. The above plot shows the results for the test at engine lambda = 0.8 and spark timing = 10 degrees aTDC. In this test, sizeable particle reductions were achieved for all particle sizes and all exhaust lambda values. The shape of the baseline curve was noticeably different for this test compared to the lower engine enrichment tests. Concentrations of small particles (23-60 nm) were lower at this test condition as compared to the previous test at the same spark timing and engine lambda = 0.9. Concentrations of mid-sized particles were similar for both tests. The baseline for this

test shows a peak concentration in the mid-range and reduced concentrations for larger and smaller particles.

At this test condition, the lowest particle concentrations were measured for exhaust lambda = 1.05. At higher SAI rates, particle concentrations began to rise again. The exhaust temperature and CO reduction at this engine condition were also maximums at exhaust lambda = 1.05. This was explained as being the result of the dilution effect of excess air present at higher SAI rates. This phenomenon is discussed more thoroughly later in the study.

3.3.4 Particle Distribution: Engine Lambda=0.8, Spark=15 aTDC

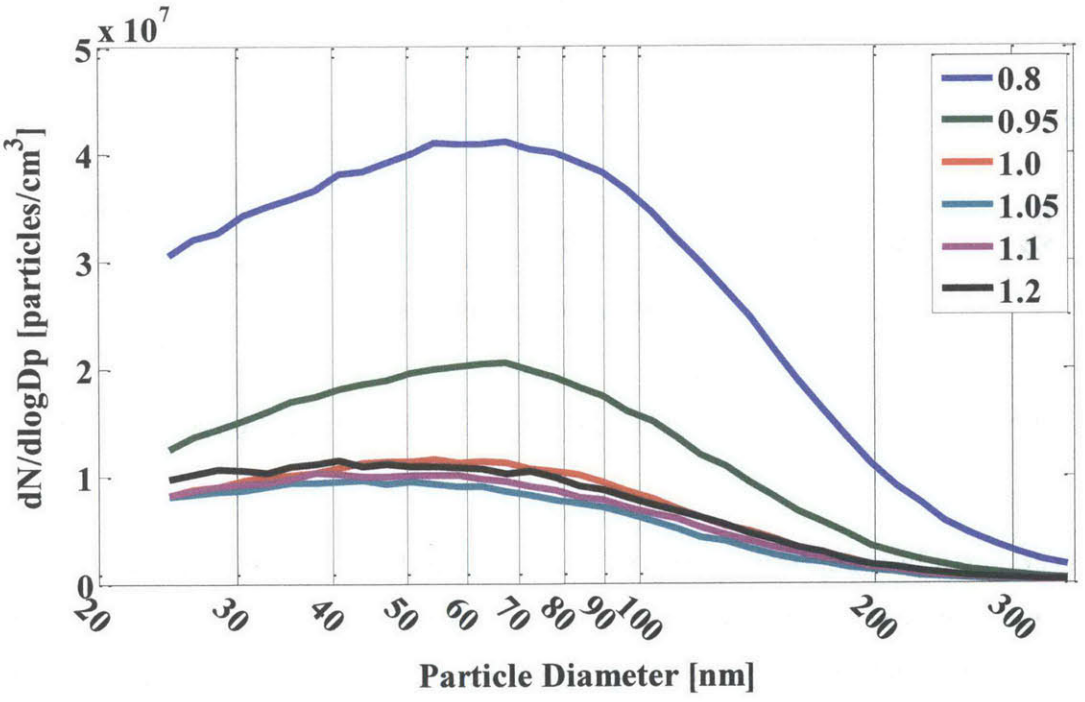

Figure 3-12: Particle distribution for engine lambda=0.8, spark=15 aTDC

Particle distributions for the final test are shown above. The engine conditions for this test were engine lambda = 0.8 and spark timing = 15 degrees aTDC. The shape of

the distributions for this test were quite similar to those for the previous test at spark timing = 10 degrees aTDC. The peak particle concentration was about 1.5 times higher in this case. As with the engine lambda = 0.9 tests, the higher baseline PM emissions are a result of the later spark timing. This test showed a decrease in particle concentrations for the entire spectrum with the addition of secondary air. The reductions were greatest for the case with exhaust lambda = 1.05. Particle concentrations increased as additional secondary air was added. This phenomenon was also noticed in the previous test.

3.3.5 Total Particulate Matter Reduction Tables

The particle distributions presented above are useful for observing the effects of SAI on the shape of the distributions. It is useful to observe the effects of SAI on total particle number or total particle volume. For this purpose, the particle results will be presented here in tabular form. Each table presents values for the percent reduction of PM for various exhaust lambdas. The reductions are relative to the tests without any SAI for each engine condition. The first table presents total particle number reductions. Total particle number is given as the cumulative particle concentrations for all particle sizes. The second table presents total particle volume reductions. Particle volume is calculated by determining an average particle volume for each measurement bin by using the particle diameter of each bin. Total particle volume is then the cumulative volume concentration for all particle sizes. This measurement is much more heavily weighted by larger particles because they have a much higher volume than the smallest measured particles. For the purposes of this study, particle volume effects are used to predict particle mass effects. This prediction depends on the assumption that particle density is constant for all PM.

Particle Number Reduction [%]						
		Exhaust Lambda				
Engine Lambda	**Spark Timing [deg. aTDC]**	**0.95**	**1**	**1.05**	**1.1**	**1.2**
0.9	**10**	4.7	9.4	21.9	23.2	29.5
0.9	**15**	7.8	30.7	44.7	47.8	50.8
0.8	**10**	47.1	61.5	65.2	57.1	49.4
0.8	**15**	55.5	74.9	79.7	77.8	74.9

Table 3-2: Particle number reduction percent for all tests

Particle Volume Reduction [%]						
		Exhaust Lambda				
Engine Lambda	**Spark Timing [deg. aTDC]**	**0.95**	**1**	**1.05**	**1.1**	**1.2**
0.9	**10**	11.2	18.2	32.3	30.0	37.6
0.9	**15**	4.8	30.8	42.7	47.1	52.3
0.8	**10**	65.4	76.1	79.4	71.2	62.1
0.8	**15**	66.0	82.8	88.1	85.8	82.5

Table 3-3: Particle volume reduction percent for all tests

The above tables show that sizeable reductions in both particle number and particle volume were achieved for almost all tests. For the tests at engine lambda = 0.9, reductions increased as SAI rate increased. These reductions were much smaller than those at engine lambda = 0.8. For tests at the higher engine enrichment, higher reductions of both particle number and volume were observed. This is likely due to more robust oxidation and higher energy release in the exhaust. For the engine lambda = 0.8 tests, PM reductions for both number and volume were maximized at an exhaust

lambda = 1.05. The relation of PM reduction to SAI rate and exhaust energy release will be investigated in the next section.

3.3.6 Particle Matter Reduction Analysis

The stated goal of this study was to investigate the effects of SAI on PM emissions. The data presented so far has shown that heat release in the exhaust system with SAI was achieved for all tests. Exhaust oxidation yielded higher exhaust stream temperature and PM reductions were seen for all tests of SAI. What remains to be investigated is the relation between these effects. Some general trends have been observed thus far. For instance, in the engine lambda = 0.8 tests, exhaust temperatures, CO reduction, and PM reduction all peaked in the exhaust lambda = 1.05 tests. This and similar trends are investigated in this section.

Figure 3-13 shows the total particle number concentration as a function of exhaust lambda for all tests. For both of the engine lambda = 0.9 tests, particle number decreased as the SAI rate increased. Minimum particle number emissions were achieved at an exhaust lambda of 1.2 for both of these tests. This was an effect of better mixing of exhaust products and secondary air within the exhaust port at higher air rates. This mixing effect was also beneficial for total CO reduction as was discussed in section 3.2. At exhaust lambda of 1.0 or greater, particle number concentrations were similar for both engine lambda = 0.9 conditions.

For the engine lambda = 0.8 tests, particle number concentration was a minimum at exhaust lambda = 1.05. It was noted previously that CO reduction was maximized with exhaust lambda = 1.05 for these conditions. For higher air rates, the excess air dilutes the exhaust mixture and reduces temperatures and oxidation rates. At exhaust lambda of 1.0 and greater, total particle number concentrations are quite similar for both engine lambda = 0.8 tests.

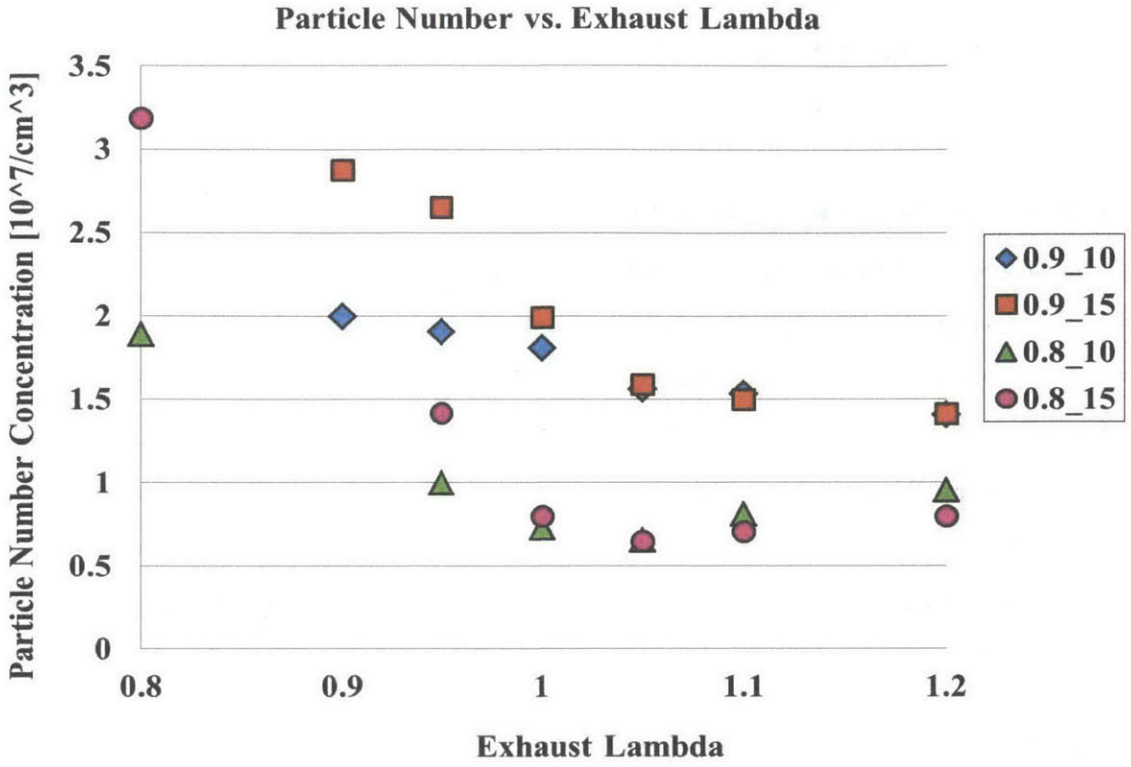

Figure 3-13: Particle number concentration vs. exhaust lambda for all tests

Figure 3-14 shows total particle volume concentration as a function of exhaust lambda. Many of the same trends for particle number were seen for particle volume. For both tests with engine lambda = 0.9, particle volume was minimized at the highest SAI rate (exhaust lambda = 1.2). For the tests with engine lambda = 0.8, particle volume was minimized with an exhaust lambda of 1.05. As with particle numbers, particle volumes for the highest SAI rates were mostly independent of spark timing and more dependent on engine lambda.

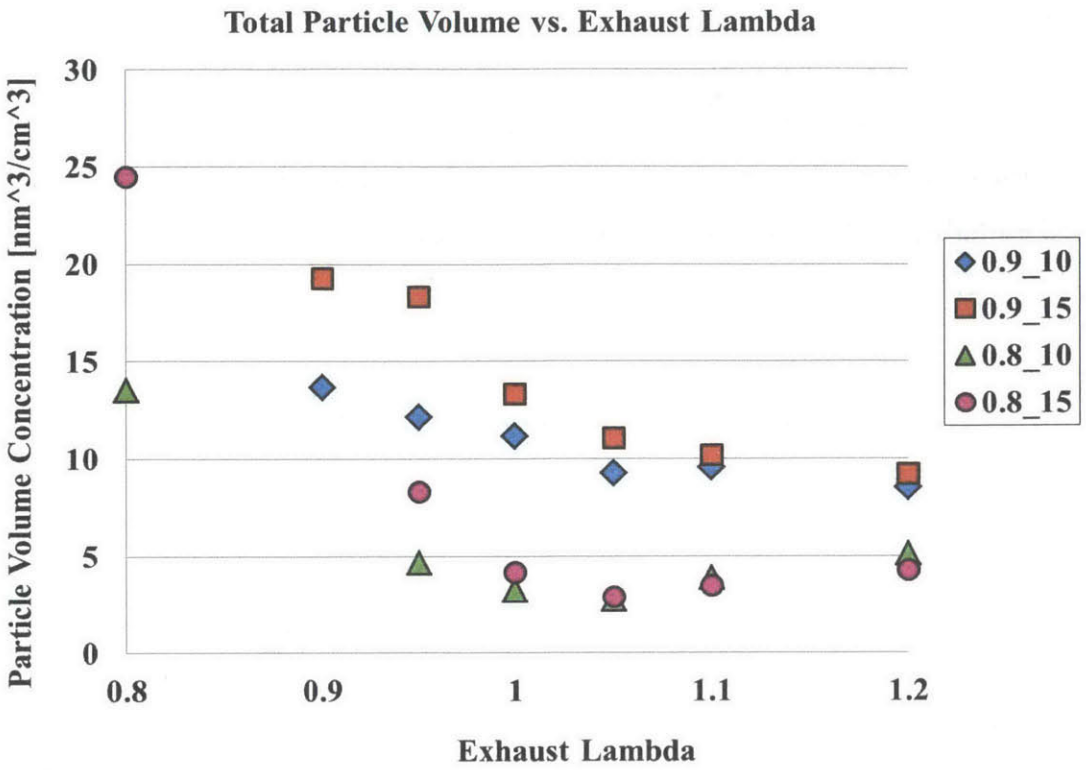

Figure 3-14: Particle volume concentration vs. exhaust lambda for all tests

It has been previously noted that both PM emissions reduction and CO reduction followed similar trends with respect to SAI rate (exhaust lambda). To investigate these trends, PM reduction was plotted as a function of the estimated, specific enthalpy release from oxidation in the exhaust system. Specific enthalpy release was estimated as follows:

$$Enthalpy\ Release\ \left[\frac{kJ}{kg_{exhaust}}\right] = CO\ Reduction\ Fraction * Exhaust\ Enthalpy\ \left[\frac{kJ}{kg_{exhaust}}\right]$$

The estimated values of exhaust chemical enthalpy for each engine condition are given in Table 2-3. Exhaust chemical enthalpy estimates include only the engine-out products and not the SAI flow. The specific chemical enthalpy is given as per kilogram of engine-out exhaust flow. Engine-out exhaust flow was constant for all SAI rates at a particular engine condition. Exhaust enthalpy values for engine lambda = 0.8 tests were

about double the enthalpy values for engine lambda = 0.9 tests. The higher enrichment level produced higher concentrations of CO, H2, and HC. It was noted that total CO reduction was not vastly different for tests at the two different enrichment levels. However, the difference in exhaust chemical enthalpy led to a large difference in the estimated enthalpy release at different enrichment levels.

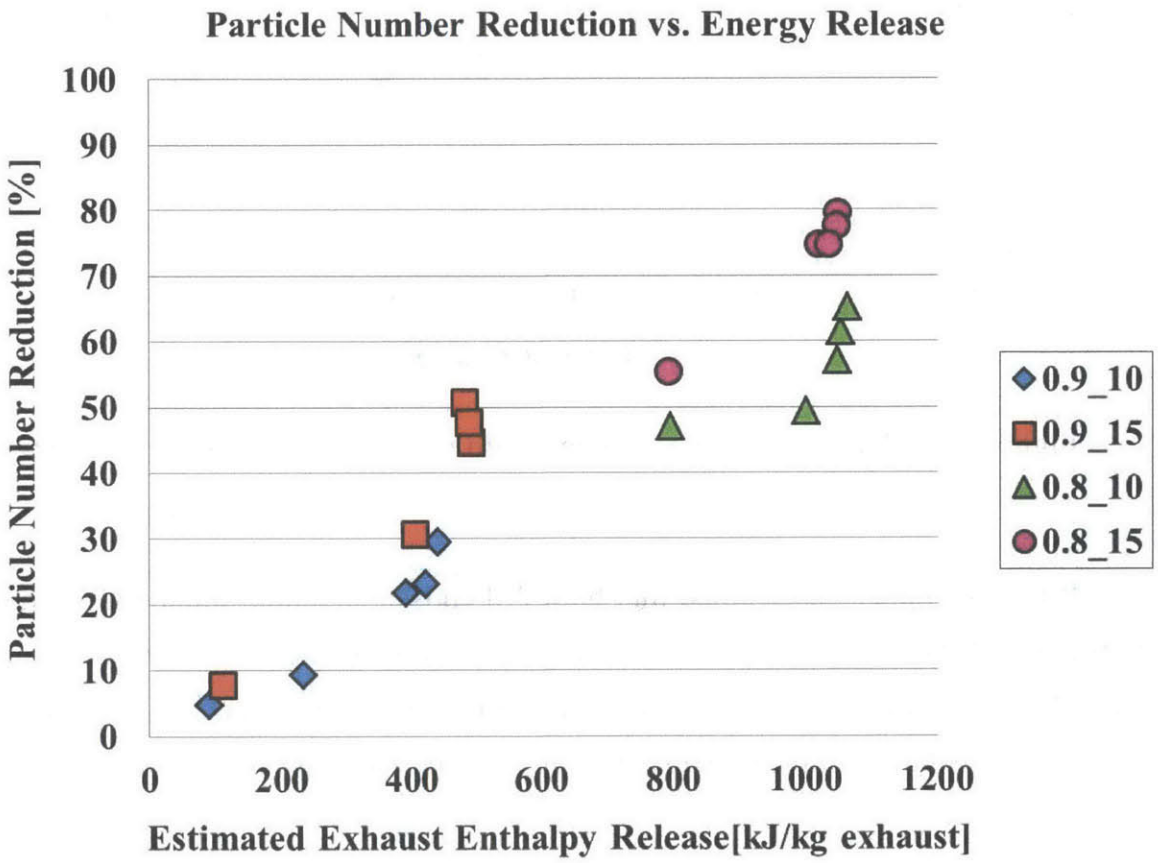

Figure 3-15: Particle number reduction vs. exhaust enthalpy release

Figure 3-15 and Figure 3-16 show particle number reduction and particle volume reduction as a function of exhaust enthalpy release. They both show similar trends. Both plots illustrate a good correlation between PM reduction values and exhaust

enthalpy release. This indicates that the amount of PM reduced within the exhaust system is related to the amount of enthalpy released through the use of SAI.

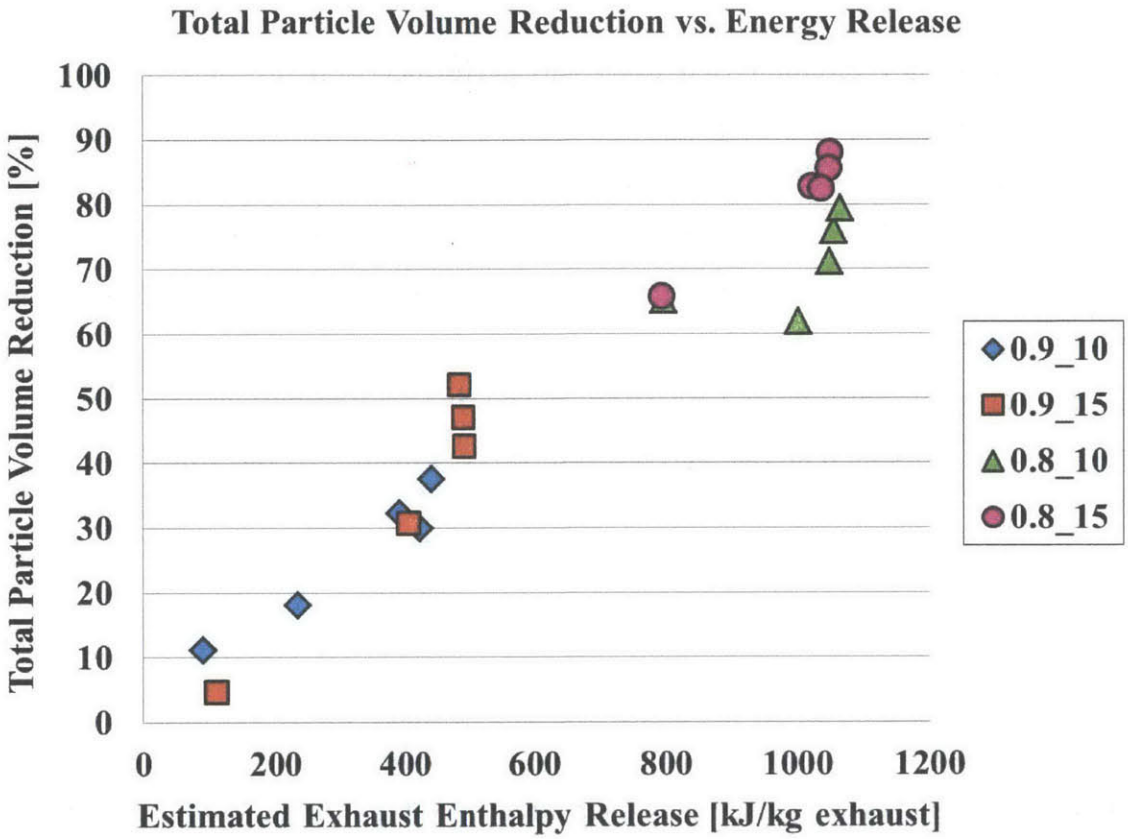

Figure 3-16: Particle volume reduction vs. exhaust enthalpy release

Chapter 4: Summary and Conclusions

4.1 Overview

An experimental, engine based study was performed to investigate the effects of secondary air injection (SAI) on particulate matter (PM) emissions. SAI was developed in the 1970s and has been extensively studied as a strategy to reduce hydrocarbon emissions. No study thus far has studied SAI specifically with regards to PM emissions. Tests were performed using a 2.0 L, DISI, turbocharged GM LNF engine. PM emissions measurements, exhaust stream temperatures, and engine performance data was collected for various engine conditions and SAI flow rates. This section will summarize the results of the testing and analysis and present the conclusions of the study.

4.2 Exhaust Stream Temperature

Exhaust stream temperature was measured at five locations within the exhaust system for all tests. Temperatures were measured by k-type thermocouples at the locations illustrated in Figure 2-1and Figure 2-5. These temperatures were useful in determining the location where SAI oxidation takes place within the exhaust system. They also enabled an estimate of the extent of oxidation. Exhaust stream temperatures with SAI were typically compared with baseline temperatures without SAI. Temperature increases were observed for all engine conditions and all SAI flow rates. This indicated that SAI enabled oxidation of exhaust products for all of the tested conditions. Peak temperatures within the exhaust system were observed to be higher for tests with later spark timing. This was the result of two effects. Engine-out exhaust temperatures are higher with later spark timing. These higher temperatures in turn led to more complete oxidation of combustible exhaust products and therefore higher heat release. Temperature increases relative to the baseline cases were much higher for

conditions with higher engine enrichment. The tests with engine lambda = 0.8 had about double the exhaust chemical enthalpy as tests with engine lambda = 0.9. Higher release of chemical enthalpy within the exhaust led to substantially higher temperature increases. For all tests, temperature increases were highest for exhaust lambda of 1.0 or 1.05. Higher SAI rates tended to facilitate better mixing within the exhaust port and to enhance oxidation. Higher SAI rates also led to excess air in the exhaust which lowered temperatures due to the effect of dilution. The cases with exhaust lambda of 1.0 or 1.05 provided adequate mixing without the dilution effects of excess air.

4.3 Oxidation Analysis

An oxidation analysis was performed to determine the amount and location of oxidation with SAI within the exhaust system. Total oxidation was based on the reduction of CO from the baseline tests, assuming that the extent of oxidation of HC and H2 are similar to that of CO. The oxidation within individual zones was determined with an energy balance. The oxidation analysis provided some insight into the effects of SAI rate on the oxidation reaction within the exhaust. The majority of overall oxidation occurred in the exhaust port (Zone 0) for all engine conditions and all SAI rates. The amount of oxidation in the port increased with increasing SAI rate for all tests. This was an effect of better mixing within the port when more air was injected. Of the four engine conditions tested, three of them resulted in a peak CO reduction of 95% or greater. For these tests with high overall oxidation rates, CO reduction peaked with an exhaust lambda of 1.05. Although higher SAI rates gave better oxidation within the port, they also led to more excess air. The excess air cooled the exhaust mixture and limited overall oxidation. SAI rate was also seen to affect the location of oxidation within the exhaust system. Higher SAI rates increased oxidation in the port but reduced oxidation further downstream.

4.4 Particulate Matter Emissions

The primary objective of this study was to investigate the effects of SAI on PM emissions. Measured PM emissions were presented in several ways to investigate different aspects of PM reduction with SAI. Particle distribution plots showed that substantial PM reductions were achieved with the use of SAI. These reductions occurred for all particle sizes but reductions were slightly larger for smaller particles. The shape of the particle distributions remained mostly unchanged as PM emissions were reduced. PM reductions were also tabulated as percent reductions for total particle number and total particle volume. In this format it was easier to identify trends with SAI rate and exhaust enthalpy release. For tests with engine lambda = 0.9, both particle number and particle volume were minimized at exhaust lambda = 1.2. This was likely an effect of better oxidation due to faster mixing in the port at higher SAI rates. Mixing was a larger factor at the lower engine enrichment level because the exhaust chemical enthalpy was reduced by half as compared to the higher enrichment tests. For tests with engine lambda = 0.8, particle number and particle volume were minimized at exhaust lambda = 1.05. PM emissions increased for higher SAI rates. This was an effect of the excess air in the exhaust at high SAI rates. Although mixing in the port was improved, overall oxidation was decreased due to the dilution effect of the excess air.

The relationship between PM reduction and exhaust enthalpy release was particularly interesting. It was observed that both particle number and particle volume reduction correlated quite well with the estimated enthalpy release within the exhaust. This indicates that PM reduction with SAI is related to the amount of enthalpy released within the exhaust. In the introduction it was noted that other studies have reported a large reduction in PM across three-way catalysts due to the oxidation of volatile particles. One study found that the catalyst reduced PM for all particle sizes. They suspected that volatiles likely exist throughout the size spectrum, both as individual particles and as condensate absorbed by larger soot particles [22]. In the current study, the volatile portion of PM was not removed before measurement. It is therefore possible

that the reduction of PM with SAI was due to the oxidation of the volatile portion of PM. Because the sampling system is heated to 200°C to prevent homogeneous nucleation, there should not be particles composed solely of volatile species. To attribute the PM reductions only to the oxidation of volatiles, it would have to be shown that volatiles existed throughout the particle spectrum as condensate absorbed onto the surface of other particles.

Another potential contributor to the measured PM reduction is the oxidation of soot particles. It was explained in the introduction that direct oxidation of soot particles is unlikely because temperatures in the exhaust are relatively low for typical soot oxidation reactions. It was also noted that soot oxidation can be related to the presence of OH radicals [21]. The oxidation of CO, H2, and HC within the exhaust system would produce OH radicals. It is possible that the formation of OH radicals from oxidation within the exhaust system is related to the reduction of PM with SAI. The correlation of PM reduction to exhaust enthalpy release would fit well with this explanation.

4.5 Conclusions

The objective of this study was to investigate the effects of secondary air injection on particulate matter emissions. Experimental, engine-based testing was successfully completed towards this end. The results of this testing are summarized below.

- The highest exhaust temperatures were achieved with exhaust lambda = 1.0 or 1.05 for engine lambda of 0.8 and 0.9. Temperatures were reduced at higher SAI rates due to the dilution effect of excess air.
- The majority of oxidation occurred within the exhaust port. Increased SAI rate led to higher oxidation in the exhaust port for all tests. This was attributed to better mixing within the port at blowdown due to more air being present.

- High SAI rates reduced the amount of oxidation that occurred in the exhaust downstream of the exhaust port. The presence of excess air reduced temperatures and slowed the rate of oxidation.

- CO reduction peaked for exhaust lambda = 1.05 for three of the four engine conditions. This was a result of balancing the effects of better mixing from higher SAI rates and the dilution effect of excess air.

- Particulate matter emissions were reduced for the engine conditions and SAI rates that were tested. Particle distributions show that particle concentrations were reduced across the size spectrum.

- The largest particle reductions for tests with engine lambda = 0.9 were achieved at an exhaust lambda = 1.2. The largest particle reductions for tests with engine lambda = 0.8 were achieved at an exhaust lambda = 1.05. This is due to the effects of better mixing and the dilution effect with higher air rates.

- Particle matter reductions correlated well with exhaust energy release. This is an interesting result that indicates PM reduction is related to the amount of oxidation that occurs within the exhaust.

- Further investigation is needed to determine the relative amount of oxidation of the condensed volatiles versus carbonaceous mass.

Bibliography

[1] R. M. Heck and R. J. Farruto, Catalytic Air Pollution Control, New York: Van Nostrand Reinhold, 1995.

[2] J. McCreanor, P. Cullinan, M. Nieuwenhuijsen, J. Stewart-Evans, E. Malliarou, L. Jarup, R. Harrington, M. Svartengren, I.-K. Han, P. Ohman-Strickland, K. F. Chung and J. Zhang, "Respiratory effects of exposure to diesel traffic in persons with asthma," *New England Journal of Medicine,* 2007.

[3] "Air Pollution and the Clean Air Act," United States Environmental Protection Agency, 15 August 2013. [Online]. Available: http://epa.gov/air/caa/. [Accessed 6 January 2014].

[4] United States Environmental Protection Agency, "Emission Facts: The History of Reducing Tailpipe Emissions," 1999.

[5] EPA Office of Transportation and Air Quality, "Light-Duty Truck--Tier 0, Tier 1, and Clean Fuel Exhaust Emission Standards," United States Environmental Protection Agency, 18 December 2012. [Online]. Available: http://www.epa.gov/otaq/standards/light-duty/tiers0-1-mdvstds.htm. [Accessed 6 January 2014].

[6] EPA Office of Transportation and Air Quality, "Light-Duty Vehicle, Light-Duty Truck, and Medium-Duty Passenger Vehicle--Tier 2 Exhaust Emission Standards," United States Environmental Protection Agency, 14 November 2012. [Online]. Available: http://www.epa.gov/otaq/standards/light-duty/tier2stds.htm. [Accessed 6 January 2014].

[7] DieselNet, "Cars and Light-Duty Trucks-Tier 3," March 2013. [Online]. Available: http://dieselnet.com/standards/us/ld_t3.php. [Accessed 6 January 2014].

[8] "Commission Regulation (EU) No. 459/2012," *Official Journal of the European Union,* 2012.

[9] J. B. Heywood, Internal Combustion Engine Fundamentals, McGraw-Hill, 1988.

[10] H. Santoso and W. K. Cheng, "MIxture Preparation and Hydrocarbon Emission Behaviors in the First Cycle of SI Engine Cranking," *SAE International,* no. 2002-

01-2805, 2002.

[11] R. Herrin, "The Importance of Secondary Air Mixing in Exhaust Thermal Reactor Systems," *SAE International,* no. 750174, 1975.

[12] F. Zhao and M. Borland, "Secondary Air Injection for Improvin Catalyst Light-Off Performance," in *Technologies for Near-Zero-Emission Gasoline-Powered Vehicles*, SAE International, 2006, pp. 173-204.

[13] I. Whelan, W. Smith and D. Timoney, "The Effect of Engine Operating Conditions on Engine-out Particulate Matter from a Gasoline Direct-injection Engine during Cold-start," *SAE International,* no. 2012-01-1711, 2012.

[14] D. Sabathil, A. Koenigstein, P. Schaffner, J. Fritzsche and A. Doehler, "The Influence of DISI Engine Operating Parameters on Particle Number Emissions," *SAE International,* no. 2011-01-0143, 2011.

[15] S. Sakai, M. Hageman and D. Rothamer, "Effect of Equivalence Ratio on the Particluate Emissions from a Spark-Ignited, Direct-Injected Gasoline Engine," *SAE International,* no. 2013-01-1560, 2013.

[16] L. Chen, M. Braisher, A. Crossley, R. Stone and D. Richardson, "The Influence of Ethanol Blends on Particulate Matter Emissions from Gasoline Direct Injection Engines," *SAE International,* no. 2010-01-0793, 2010.

[17] K. Aikawa, T. Sakurai and J. J. Jetter, "Development of a Predictive Model for Gasoline," *SAE International,* no. 2010-01-2115, 2010.

[18] P. Price, R. Stone, D. OudeNijeweme and X. Chen, "Cold Start Particulate Emissions from a Second," *SAE International,* no. 2007-01-1931, 2007.

[19] J. Nagle and R. F. Strickland-Constable, "Oxidation of Carbon between 1000-2000 C," in *Proceedings of the Fifth Carbon Conference*, Oxford, 1962.

[20] H. Song, N. Ladommatos and H. Zhao, "Diesel Soot Oxidation under Controlled Conditions," *SAE International,* no. 2001-01-3673, 2001.

[21] B. S. Haynes and H. G. Wagner, "Soot Formation," *Progress in Energy and Combustion Science,* vol. 7, no. 4, pp. 229-273, 1981.

[22] P. Ericcson and A. Samson, "Characterization of Particulate Emissions Propogating

in the Exhaust Line for Spark Ignited Engines," *SAE International,* no. 2009-01-2654, 2009.

[23] I. Whelan, D. Timoney, W. Smith and S. Samuel, "The Effect of a Three-Way Catalytic Converter on Particulate," *SAE International,* no. 2013-01-1305, 2013.

[24] I. Whelan, S. Samuel and A. Hassaneen, "Investigation into the Role of Catalytic Converters," *SAE International,* no. 2010-01-1572, 2010.

[25] K. Kollmann, J. Abthoff, W. Zahn, H. Bischof and J. Giarhre, "Secondary Air Injection with a New Developed Electrical Blower for Reduced Exhaust Emissions," *SAE International,* no. 940472, 1994.

[26] D. Lee, "Effects of Secondary Air Injection During Cold Start of SI Engines," Massachusetts Institute of Technology, 2010.

[27] J. Ketterer, "Soot Formation in Direct Injection Spark Ignition Engines Under Cold-Idle Operating Conditions," Massachusetts Institute of Technology, 2014.

[28] *Model 3934 SMPS (Scanning Mobility Particle Sizer) Instruction Manual, Revision D,* TSI Incorporated, 1996.

[29] K. Cedrone, "Control Strategy for Hydrocarbon Emissions in Turbocharged Direct Injection Spark Ignition Engines During Cold-Start," Massachusetts Institute of Technology, 2013.

[30] TSI Incorporated, "Aerosol Statistics Lognormal Distributions and dN/dlogDp: Application Note PR-001," TSI Incorporated, 2010.

[31] Cambustion, "Fast FID Principles," [Online]. Available: http://www.cambustion.com/products/hfr500/fast-fid-principles. [Accessed 6 January 2014].

[32] J. L. Hernandez, G. Herding, A. Carstensen and U. Spicher, "A Study of the Thermochemical Conditions in the Exhaust Manifold Using Secondary Air in a 2.0 L Engine," *SAE International,* no. 2002-01-1676, 2002.